5-2017

Salinic to Neoacadian Deformation within the Migmatite Zone of the Central Maine Belt in Western Maine

Erik James Divan
Bates College, edivan@bates.edu

Salinic to Neoacadian Deformation within the Migmatite Zone of the Central Maine Belt in Western Maine

Bates College Department of Geology Departmental Thesis

Presented to the Faculty of the Department of Geology, Bates College, in partial fulfillment of the requirements for the Degree of Bachelor of Science

By

Erik James Divan

Lewiston, Maine

April 7th, 2017

SALINIC TO NEOACADIAN DEFORMATION WITHIN THE MIGMATITE ZONE OF THE CENTRAL MAINE BELT IN WESTERN MAINE

Divan, Erik, J, Wheatcroft, Audrey, Eusden, Dykstra, Geology, Bates College, 44 Campus Ave, Lewiston, ME 04240, edivan@bates.edu

Detailed bedrock mapping coupled with new geochronology in the southern part of the Gilead 7.5' Quadrangle in Western Maine has revealed at least three phases of Salinic through Neoacadian deformation. The geology of the study area is dominated by the migmatized Silurian Rangeley, Perry Mtn. (?), and Smalls Falls Formations of the Central Maine Belt (CMB), which are intruded by quartz diorites from the Piscataquis Volcanic Arc, two-mica granites, and pegmatite. All of the metasedimentary rocks are stromatic migmatites, part of the Migmatite-Granite Complex (Solar and Tomascak, 2016). The geochronology (Wheatcroft, 2017) brackets the cycle of deposition, metamorphism, migmatization, and deformation to between circa 435 Ma. to 352 Ma.

D_1 is represented by cryptic pre-metamorphic faults that offset and truncate the stratigraphic units. Pre-metamorphic faults are observed outside of the study area in a contiguous section to the north. These faults are likely Salinic in age and developed synchronous with deposition or circa 435 Ma..

D_2 deformation is characterized by nappe-scale, isoclinal folding of unknown vergence where bedding, S_0, is parallel to schistosity, S_2. Only a few F_2 folds are present in the study area and in these places bedding, S_0, is antiparallel to S_2 schistosity. The gray schists and quartzites above Bog Brook in the study area preserve this fabric relationship and suggest the presence of a macroscale F_2 hinge zone. The extensive migmatization has obscured most of the D_2 fabrics that are likely Early Acadian in age.

D_3 deformation is characterized by numerous open, reclined, upright to overturned, macroscopic folds with limbs striking 245, 87 and 345, 62, a calculated inter-limb angle of 83°, and a hinge line trend and plunge of 55, 60. Mesoscopic D_3 folds of the composite S_0/S_2 fabrics are common but of diverse fold orientations due to the migmatization. The S_3 axial planar cleavage is characterized by a zonal crenulation in the F_3 mesoscale folds. The stratigraphic age assignment supported by lithologic correlation and new detrital zircon geochronology suggests the stratigraphy is inverted due to D_2 isoclinal folding. As such the D_3 folds are best characterized as antiformal synclines and synformal anticlines and are likely of Late Acadian or Neoacadian in age (pre-352 Ma.).

Acknowledgements

I would like to thank the Bates College Department of Geology for supporting me throughout my undergraduate geology career, and for offering frequent and constructive feedback on this project, and so many others. It has truly been a pleasure to explore the complex geology of Maine with the talented professionals that continue to guide young students and stoke new passion for the field of each and every year.

This project was funded by donations generously provided by the Billings Fund, the Hoffman Foundation, the Bates Student Research Foundation, and the Bates College Department of Geology. Without the support of these institutions, as well the support of Mike Retelle and Dykstra Eusden, the completion and presentation of this research at multiple professional conferences would not have been possible. I would also like to include a special thanks to the wonderful staff at AMCs Camp Dodge. Without their generous hospitality, it would not have been possible for my thesis partner, Audrey Wheatcroft, and me to complete our respective projects.

I would like to thank my coach, Peter Steenstra, for pushing me to be a successful student athlete, and for showing me the merits of hard work both on and off the water. Rowing at Bates College is an experience that has, and continues to shape me as a student athlete and as a person.

To my thesis and academic advisor, Dykstra Eusden, I would like to extend to you my sincere appreciation for all of the help you have given me throughout my academic career. Taking my first geology class with you my sophomore year made me passionate about the exciting and diverse opportunities available to a field geologist in Maine. To say that my thesis would not have been possible without you is a gross understatement. Thank you for making the time and having the patience to allow me to be a successful student.

To my fellow classmates I would like to thank you for your support throughout my senior year. In particular I would like to thank my friend Ian Hillenbrand for the thoughtful insight that he is always willing to provide and for his constant encouragement throughout the process of this thesis. I would also like to thank Adam Rintell for the coffee runs and thesis companionship on many an early Sunday morning. Thank you for helping to make this possible.

Finally, I would like to thank my parents, Jim and Teresa Divan, who have given me their unquestioning support and love for my entire life. Without them I would have none of the wonderful opportunities that I have been afforded. I cannot thank them enough for being a positive influence on me and for being a shining example of what it is to be good people and wonderful parents.

Contents

Abstract…………………………………………………………………………………………….ii

Acknowledgements…………………………………………………………………………...iii

Introduction……………………………………………………………………………………...1

Glacial History………………………………………………………………………….3

General Purpose………………………………………………………………………...4

Previous Studies………………………………………………………………………...4

Depositional and Deformations Setting………………………………………………...5

Field Structures…………………………………………………………………………7

Metamorphism………………………………………………………………………….8

Methods……………………………………………………………………………………….10

Field Mapping………………………………………………………………………….10

Thin Section Preparation……………………………………………………………….11

Thin Section Analysis………………………………………………………………….11

Stereonet Generation and Analysis…………………………………………………….12

Fold Classifications…………………………………………………………………….14

Cross Section…………………………………………………………………………...16

Geochronology Significance…………………………………………………………...16

Literature……………………………………………………………………………….17

Results………………………………………………………………………………………..18

Timing of Deformation………………………………………………………………...18

Salinic Deformation (D_1)…………………………………………………………………19

Acadian Folding (D_2)……………………………………………………………………..19

Neoacadian Folding (D_3)…………………………………………………………………22

Crenulations…………………………………………………………………………….30

Cross Section…………………………………………………………………………...30

Structural Map………………………………………………………………………….30

Discussion……………………………………………………………………………………….33

Local Stratigraphic Correlations……………………………………………………..33

Local Structural Correlations………………………………………………………...34

Salinic Deformation …………………………………………………………………....34

Acadian Deformation…………………………………………………………………...34

Neoacadian Deformation……………………………………………………………..35

Regional Refolding Evidence...…………………………………………………………36

Previous Interpretations…….…………………………………………………………...37

Updated Post Depositional History……………………………………………………..38

Conclusions………………………………………………………………………………....41

References……………………………………………………………………………………..42

List of Figures

Figure 1: Study area location map (Osberg et al, 1985)…………………………………………….…1

Figure 2: Surficial geology map of study area (Thompsoson et al, 1985)……………………………...3

Figure 3: Study area location (Hibbard et al, 2006)……………………………………………...5

Figure 4: Stratigraphic cross section of CMB (Bradley and O'Sullivan, 2016)……………………....5

Figure 5: Silurian to late Devonian deformation (van Staal, 2009)…………………………………..6

Figure 6: D_1 and D_2 annotated outcrop……………………………………………………………..7

Figure 7: Acadian foreland basin progression (Bradley et al, 2000)………………………………….8

Figure 8: Outcrops and field map……………………………………………………………….10

Figure 9: Lab rock saws………………………………………………………………………....11

Figure 10: Olympus BH-2 model BHSP polarizing microscope……………………………………..12

Figure 11: Raw S_0 and S_2 beta and pi diagrams………………………………………………...…12

Figure 12: Beta and pi diagrams (Taylor et al, 1997)...…....13

Figure 13: Outcrop scale crenulations…………………………………………………………..14

Figure 14: Fluety, fold angles, fold isogons, refolded folds (Fossen, 2010; Press and Seiver, 2007)..15

Figure 15: Timing of deformational events……………………………………………………..18

Figure 16: Field station 108, F_2 annotated outcrop hinge……………………………………...…..20

Figure 17: Field station 128, F_2 annotated oucrop hinge………………………………………..20

Figure 18: Bog Brook grey schist S_2 foliation………………………………………………………..20

Figure 19: Bog Brook grey schist thin section………………………………………………………..21

Figure 20: S_0&S_2 annotated contour diagram……………………………………………………...22

Figure 21: Field station 1, F_3 annotated outcrop………………………………………………...23

Figure 22: Field station 7, F_3 annotated outcrop………………………………………………...23

Figure 23: Field station 8, F_3 annotated outcrop………………………………………………...23

Figure 24: Field station 10, F_3 annotated outcrop……………………………………………….23

Figure 25: Field station 12, F_3 annotated outcrop……………………………………………….24

Figure 26: Field station 13, F_3 annotated outcrop……………………………………………….24

Figure 27: Field station 14, F_3 annotated outcrop……………………………………………………...…24
Figure 28: Field station 34, F_3 annotated outcrop…………………………………………………….…..24
Figure 29: Field station 73, F_3 annotated outcrop…………………………………………………….…..25
Figure 30: Field station 75, F_3 annotated outcrop…………………………………………………….…..25
Figure 31: Field station 89, F_3 annotated outcrop…………………………………………………….…..25
Figure 32: Field station 90, F_3 annotated outcrop…………………………………………………….…..25
Figure 33: Field station 180, F_3 annotated outcrop……………………………………………………....26
Figure 34: Field station 181, F_3 annotated outcrop…………………………………………………..…...26
Figure 35: Field station 185, F_3 annotated outcrop…………………………………………………..…26
Figure 36: Field station 190, F_3 annotated outcrop…………………………………………………..…26
Figure 37: Field station 212, F_3 annotated outcrop…………………………………………………..…27
Figure 38: Field station 264, F_3 annotated outcrop…………………………………………………..…27
Figure 39: F_3 axial plane equal area projections and contour diagram………………………………...27
Figure 40: Peaked Hill rusty schist crenulation and migmitized structures…………………………..…...29
Figure 41: Peaked Hill rusty schist thin section…………………………………………………………..29
Figure 42: Cross section…………………………………………………………………………………..31
Figure 43: Structural map…………………………………………………………………………………32
Figure 44: Stratigraphic revisions (Watermulder, 2014)…………………………………………….....33
Figure 45: Mooselookmeguntic pluton location (Solar and Tomascak, 2016)………………………....35
Figure 46: Gilead and Bethel, Maine 7.5’ quadrangle refolded nappe structure……………………....36
Figure 47: Previous syn/post depositional interpretations (Watermulder, 2014)……………………..…37
Figure 48: Silurian deformational events……………………………………………………………..…38
Figure 49: Early Devonian deformational events…………….……………………………………....39
Figure 50: Late Devonian deformational events…………………………………………………….....40

List of Tables

Table 1: Orogenic correlation chart……………………………………………………………..9

Table 2: F_3 fold data chart…………………………………………………………………………28

Introduction

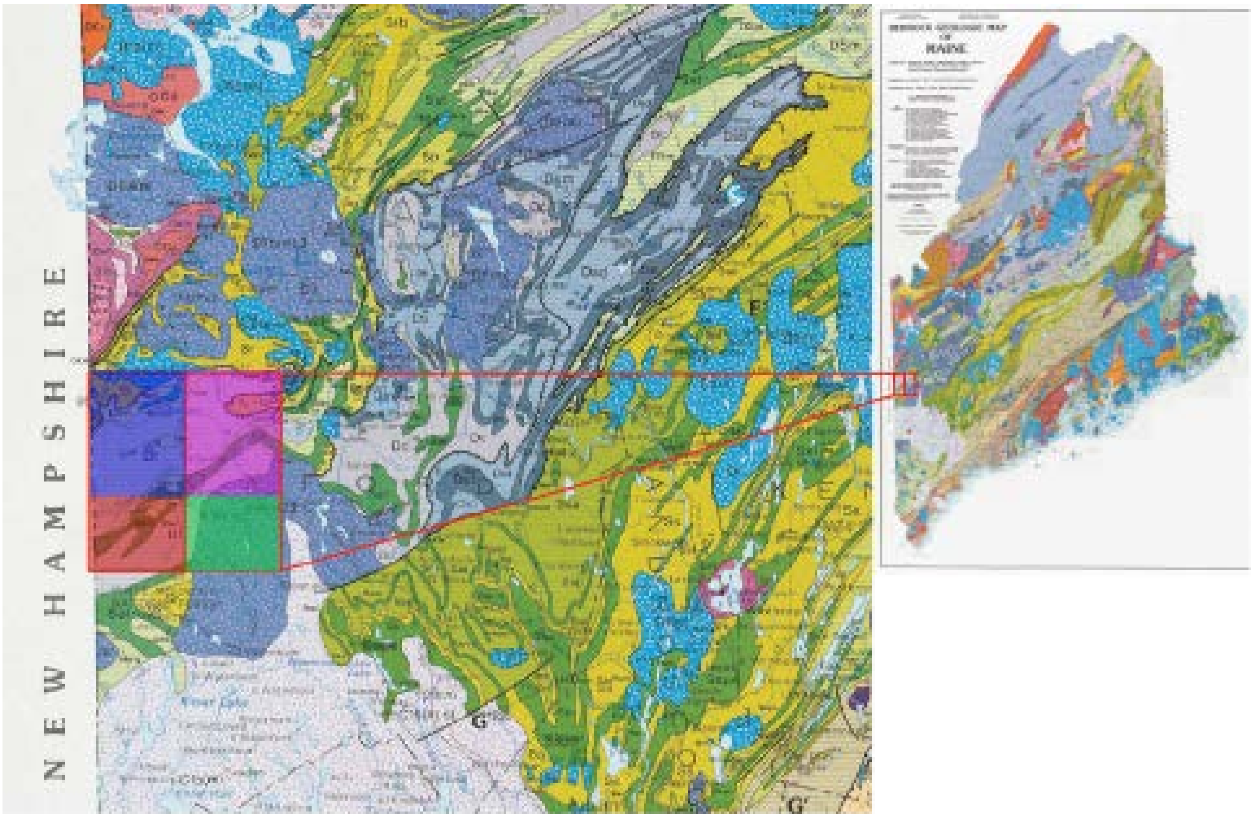

Figure 1. Project study area, highlighted in red, superimposed on Osberg et al (1985) Maine State Bedrock map. Gilead and Bethel, Maine, 7.5' quadrangles outlined. Blue and purple polygons represent study areas mapped by Watermulder (2014) and Choe (2014), and Eusden (2015) respectively. Green polygon represents currently unmapped region in Bethel, Maine 7.5' quadrangle which will be mapped in future projects.

This project focuses on providing an interpretation of the deformational history of the Northern Appalachian Mountains based on data gathered in the Gilead 7.5' quadrangle in Western Maine during the 2016 summer field season. Locals and visitors alike would benefit greatly from an increased understanding of the tectonic and deformational history of the Appalachians. A more detailed bedrock map (1:10000), showing the folds and lithology of local rock types will provide a number of societal benefits. Geologic maps are recognized as the instrument of choice for planning and executing research and decisions that involve earth science information (Resnick et al, 1987). Maps can be used to educate new homebuyers who may be concerned about the condition of the land they are relocating to. Geologic maps can also provide information on water, atmospheric and geologic hazards that may impact homeowners and their families.

Bedrock maps are the first resource used by city planners when considering zoning for developments. Resource managers looking for water, or minerals also benefit from having up to date and accurate bedrock maps. These data may also be used to support new academic models of deformation, structure, and stratigraphy, as is the case with this study, and a complimentary project conducted by Audrey Wheatcroft (2017).

The study area for this thesis is in the southern half of the Gilead 7.5’ quadrangle, shown on the current Maine State bedrock map in figure 1. The Gilead 7.5’ quadrangle is located at the western edge of the Maine state border. The Gilead 7.5’ quadrangle is adjacent to the Bethel 7.5’ quadrangle to the East, and the Shelburne 7.5’ quadrangle to the West. Previous mapping is highlighted by the blue and purple polygons, which denote the areas mapped by Sula Watermulder (2014) and Saebyul Choe (2014), and Riley and Dykstra Eusden (2015) respectively. The study area of this thesis is highlighted by the red polygon within the Gilead, Maine 7.5’ quadrangle. The green region in the southern portion of the Bethel 7.5’ quadrangle will be mapped by Dykstra Eusden and future students.

It is known from a wealth of previous research that the mountains in New England are the products of high-energy orogenesis during the late Silurian and Devonian. An updated bedrock map for the Gilead, Maine 7.5’ quadrangle can provide more detailed insight into the timing and character of these extraordinary tectonic events. Specific outcrop data gathered in the field, such as lithology, mineralogy, and structural deformation can also provide clues to the nature of these tectonic events. Detrital and crystallization ages from zircon crystals gathered from metasedimentary and plutonic units respectively can bracket the timing of orogenic events in the study area. These data can be compared to the previous extensive tectonic research (Billings and Billings, 1975; Bradley et al, 2000; Bradley and O’Sullivan, 2016; De Yoreo et al, 1989; Welling, 2001; van Staal, 2009) and used to support or refute current deformational theories.

Almost all of the study area rocks are highly migmatized due to high temperature low pressure conditions during metamorphism (De Yoreo et al, 1989; Solar and Tomasack, 2016). There are significant amounts of granites, diorites and pegmatites in the study area as well. Jointing in the region can be attributed to continental rifting that occurred during the breakup of Pangea during the Cretaceous. This jointing follows a general northeast-southwest strike, which is similar to the trend in bedrock strikes from earlier compression measured in this study (Watermulder, 2014). Folding has been previously mapped by Dykstra Eusden (2013), and will be used to further analyze the deformational history of New England in conjunction with fold data gathered in this study.

An updated bedrock and fold map of the Gilead quad has much to offer. Local deformational analysis can bolster previous deformational and structural research by providing context and timing for major orogenic events. Major features, such as folds, foliations, and faults can be correlated with specific known regional orogenic events, such as the Salinic, Acadian, NeoAcadian, and Alleghanian orogenies. A scaled cross section, bedrock map, and fold map generated from this thesis and from Audrey Wheatcroft’s (2017) thesis will provide detailed and valuable information for all those interested in learning about the geologic composition and history of western Maine. Wheatcroft’s (2017) thesis will provide a bedrock unit map and analysis of the stratigraphy of the Gilead, Maine 7.5’ quadrangle. This thesis will focus on the deformational history and structure of the Gilead, Maine 7.5’ quadrangle and will contextualize local orogenic timing with previous research.

Glacial History

Glaciation and subsequent deglaciation has had a major impact on the surficial geology of New England and therefore deserves acknowledgement in this thesis. Much of the landscape that is not simply exposed bedrock is glacial till. Knowledge of glacial retreat direction in New England was key in optimizing potential bedrock-rich locations during fieldwork, so as to avoid till deposits that would obscure bedrock. Glacial striations in the Gilead-Shelburne region of the Androscoggin Valley show a flow direction which is parallel to the valley itself. Westward glacial retreat in Gilead is indicated by meltwater channels carved on hillsides, as well as ice contact sands and gravel deposits along both sides of the Androscoggin Valley (Thompson et al, 2014).

The features that we observe were attributed to the retreat of the Laurentide ice sheet 14ka B.P (Thompson and Fowler, 1989). As the glacier flowed eastward across the Androscoggin Valley, it left a trail of end moraines, referred to as the Androscoggin Moraine Complex. The moraines themselves are glacial diamictons composed of flowtills with interbedded silt, sand, and gravel, surrounding large angular boulders.

Alluvial fans are another glacially derived feature that make an appearance in the surficial geology of the White Mountains. Alluvial fans are sloping, fan shaped deposits of coarse gravel that formed where steep brooks met larger streams (Thompson et al, 2014). As outlined in the GSM-GSNH 2014 field guide, fan accumulation most likely occurred immediately after the disappearance of glacial ice, when the barren mountain sides and unstable sediments on slopes were vulnerable to erosion. The surficial map of this study area is shown in figure 2.

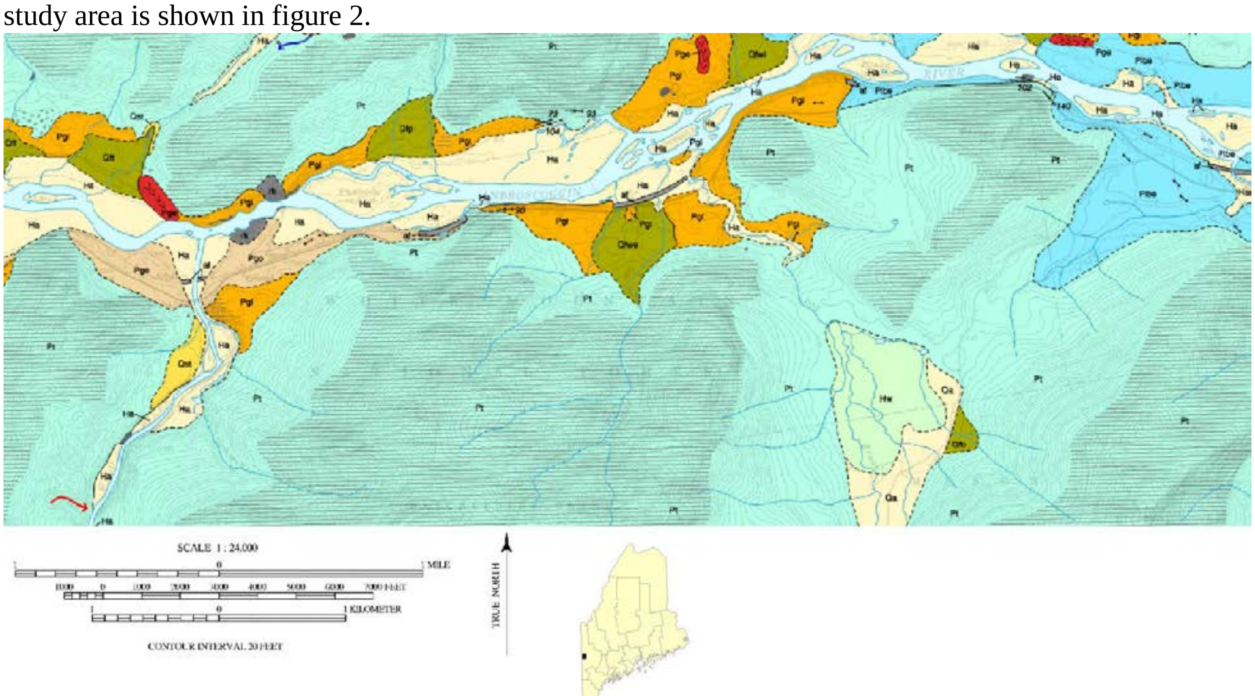

Figure 2. Surficial Geology map of southern portion of Gilead, Maine 7.5' quadrangle accessed from Maine Geological Survey. A complete map of the Gilead, Maine 7.5' quadrangle is available at the Maine Geological Survey, Department of Conservation (Thompson et al, 1985).

General Purpose

The remapping of bedrock in western Maine completed by Wheatcroft (2017) offers a more in depth look into the complex relationships between the high grade metamorphic units and igneous intrusions that the northeast has become famous for. This thesis takes a critical look at the structure of the layered and folded metamorphic rocks in the Gilead, Maine 7.5’ quadrangle, analyzing their structural relationships with fold, bedding and schist data. These data are used to provide a complete analysis of the deformational history of the local rocks in western Maine, and of overall orogenic character of New England. Specific deformational evidence found in the field have been correlated with known orogenic events. According to previous research (Billings and Billings, 1975; Bradley et al, 2000), the major tectonic events that can be identified in the rocks of northern New England were the Salinic Orogeny (~450-423ma) and the Acadian Orogeny (~420-360ma).

Constraining the timing of these tectonic events and other, later events has been made possible by using geochronology of zircons within key metasedimentary units and plutons. Detrital zircon dating of metasedimentary units has also made it possible to correlate these rocks with known stratigraphic units in the study area, such as the Rangeley, Perry Mountain, Smalls Falls, Madrid, and Littleton formations.

Intrusions in the study area have been correlated with known regional plutons (Carboniferous Sebago, Devonian Songo, and Piscataquis Volcanic Arc quartz diorites). Crystallization zircon ages from granites in the study area have been used to constrain the end of regional ductile deformation based on research completed at GeoSep Labs in Moscow, Idaho (Wheatcroft, 2017).

This study has also generated a digital fold map on ArcGIS in conjunction with the contact map created by Wheatcroft (2017). This fold map, accompanied by stereonets and a 1:1 scaled cross section are used to represent the form of macro-scale folding throughout the study area.

Many of the pre-existing interpretations of the deformation in western Maine are based on old maps and data. There has been no previous mapping in this study area at the resolution that this project and Wheatcroft (2017) project have provided (1:10000). Due to the prevalence of the logging industry and newer snow-mobile and ATV trails, there is greater access to unexplored bedrock than ever before. This new insight will not only provide the state of Maine with a more accurate bedrock map, but will also offer a more accurate analysis of the deformational time scale of western Maine and may prove to have larger implications for the overall geology of New England.

Previous Studies

The most recent map of the Maine State Bedrock was published in 1985, and was based upon data gathered from Hatch, Moench and Lyons in the 1970s. Since then, there have been multiple revisions to the bedrock near the study area, the most notable of which is the change of rocks identified as the Littleton Formation to the Rangeley Formation. Remapping done by Moench, Boudette, and Bothner in

1999 and Eusden in 2012 in the Bethel and Gilead, Maine 7.5’ quadrangles suggests that even less of the region is dominated by the Littleton Formation than expected.

Figure 3 is a 1:500000 scale map of the bedrock geology on the Eastern coast of continental United States and Canada created by Hibbard et al (2006). The units identified by Hibbard in the study area are the Madrid formation (27), the Seboomook group (32a), and the Piscataquis Volcanic Arc (32a). The maps in this study and Wheatcroft’s (2017) thesis will be drawn at a 1:10000 scale.

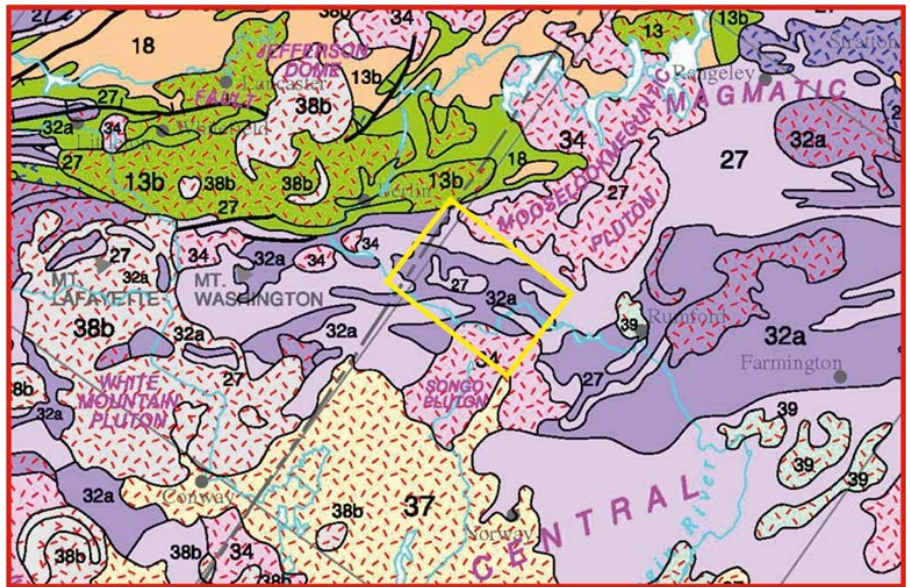

Figure 3. Bedrock geology map of the eastern seaboard of continental US and Canada, published by Hibbard et al (2006). Gilead and Bethel 7.5’ quadrangles are outlined in yellow. Significant units are the Madrid Formation (27) and the Seboomook Group, Chaleurs Group and Piscataquis Volcanic Arc (32a).

Depositional and Deformational Setting

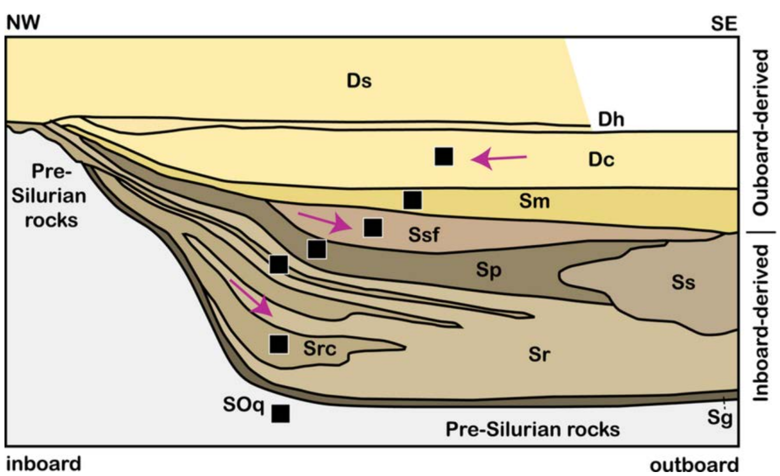

Figure 4. Cross section of Central Maine Basin (CMB) showing sedimentation direction and layering of significant stratigraphic units prior to deformation (Bradley and O’Sullivan, 2016).

The rocks in this study area are largely considered to be deposited during the Late Ordovician to the Middle Devonian (Bradley et al, 2000). These rocks were deformed by the Salinic, Acadian, and Neoacadian and Alleghenian orogenies. Figure 4 shows a recent regional cross section of the Central Maine Basin (CMB) from a 2016 publication by Bradley and O’Sullivan. Purple arrows denote sediment transport directions, differentiating the rocks as inboard derived on the bottom (NW-SE) or outboard derived overlaying (SE-NW). It has been determined that inboard strata were deposited earlier during the Late Ordovician to Silurian range, and the outboard strata were deposited later during the Devonian in the Acadian foreland basin. Stratigraphic units significant to this study area the Rangeley (Sr, Src), Smalls Falls (Ssf), and Madrid (Sm) formations. The basement unit, colored grey in figure 4 is the Silurian-Ordovician Quimbly formation, an isoclinally folded succession of siliciclastic and calcareous turbidites that is many kilometers thick (Bradley and O’Sullivan, 2016).

The inboard stratigraphic units are believed to have been deposited in a sub-marine basin prior to Acadian deformation in the CMB, shown in cross section in Figure 4. The movement of these units into the basin has been attributed to excess fluid pressure (Moench, 1970) which did not affect lower, more stable units, such as the Quimbly Formation. These units were deposited during the Silurian, with some syn-depositional deformation occurring during the Salinic, and significant post-depositional deformation during the Acadian.

The oldest of the inboard units is the Rangeley Formation, which can be identified in the field as a grey turbiditic olisostromal mélange, containing calc-silicate pods with intermittent rusty belts (Watermulder, 2014). The Smalls Falls is the youngest of the stratigraphic units with northwestern provenance. It is characterized as a rusty weathered turbiditic sandstone, and is assigned an early Ludlow deposition date based on fossils found in a similar strata in the southeast (Bradley et al, 2000).

Outboard stratigraphic units significant to this study were deposited with a more easterly provenance, and are made up of the Madrid and Littleton Formations. The Madrid Formation is described as a sandstone-dominated siliciclastic turbidite with calcareous units interbedded, particularly when approaching western Maine and New Hampshire (Bradley and Tucker, 2002). The Madrid Formation was deposited along the axis of the Acadian foreland basin sometime during the Ludlow. The Littleton Formation was deposited during the early Devonian, and is cut by the Emsian Sebec Lake pluton (Bradley et al, 2000). There are no Littleton units found in our study area, which may be due to weathering, a lack of deposition, or some combination of the two.

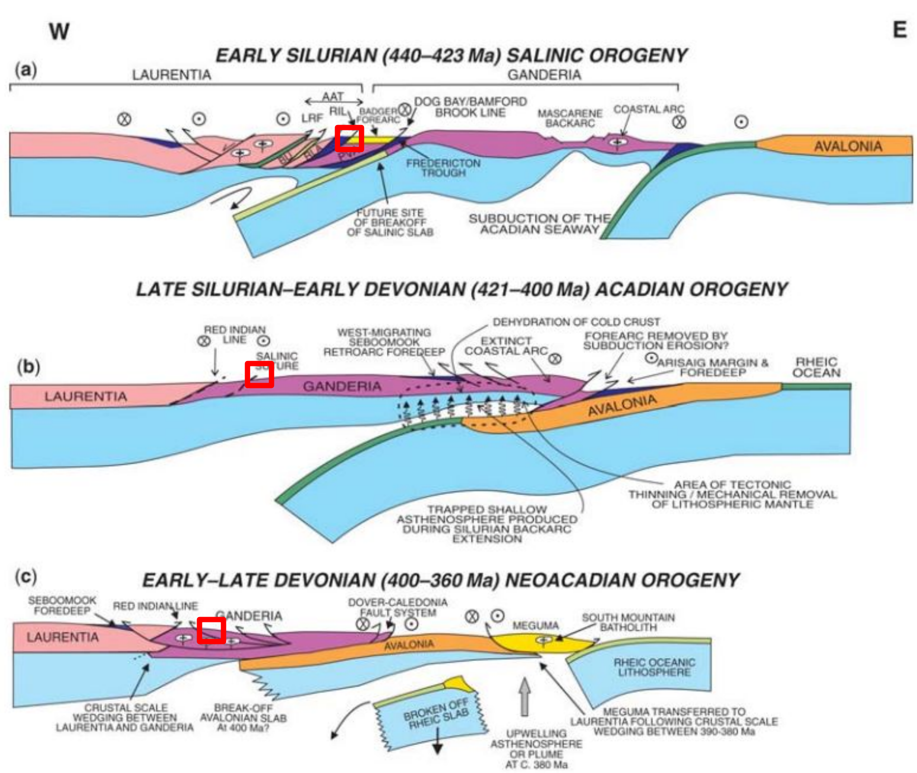

Figure 5. Continental scale regional deformation during the three major orogenic events in New England by van Staal et al (2009). Approximate location of study area shown by red outline.

Figure 5 shows a regional tectonic summary from van Staal et al (2009). The Salinic orogeny is shown in part (a) by the accretion of Gander to Laurentia. This orogeny was spurred by the closure of the back-arc Tetagouche-Exploits basin (Reusch and van Staal, 2012). (b) presents the Acadian orogeny with the subduction of Avalon and closure of the Acadian seaway. The deformational front of the Acadian orogeny did not reach western Maine until ~418ma (Bradley et al, 2000). (c) shows the accretion of Meguma, accompanied by the breakoff of the Rheic and Avalonian slabs at ~400ma. This is likely correlated with the Neoacadian or Alleghanian orogenies.

Field Structures

Field structure interpretation is of paramount importance in understanding the complex structural geology of the Gilead, Maine 7.5' quadrangle. An example of a useful identifying field structure is the previously mentioned olisostromal mélange that is characteristic of the Rangeley Formation. Features such as calc-silicate pods not only hint at the formation that these rocks are part of, but also provide evidence for their depositional environment. The sub-marine slope that served as the depositional environment of the Rangeley Formation formed layers of limestone and siliceous rocks (Watermulder, 2014). These layers were metamorphosed and fractured by tectonic events that occurred during plate subduction, giving the Rangeley Formation its characteristic calc-silicate pods. The development of an olisostromal mélange was the result of dehydration-melting reactions that occurred in the Rangeley Formation during the peak of metamorphosis. Evidence found within the Rangeley Formation for syn-depositional melting includes the presence of centimeter scale leucocratic quartz, muscovite, plagioclase pods, and the zoning of major trace elements in garnet crystals. For a more in depth description of the metamorphic processes occurring in the Rangeley Formation, refer to the study conducted by Konn, Spear and Valley in the Journal of Petrology (1997).

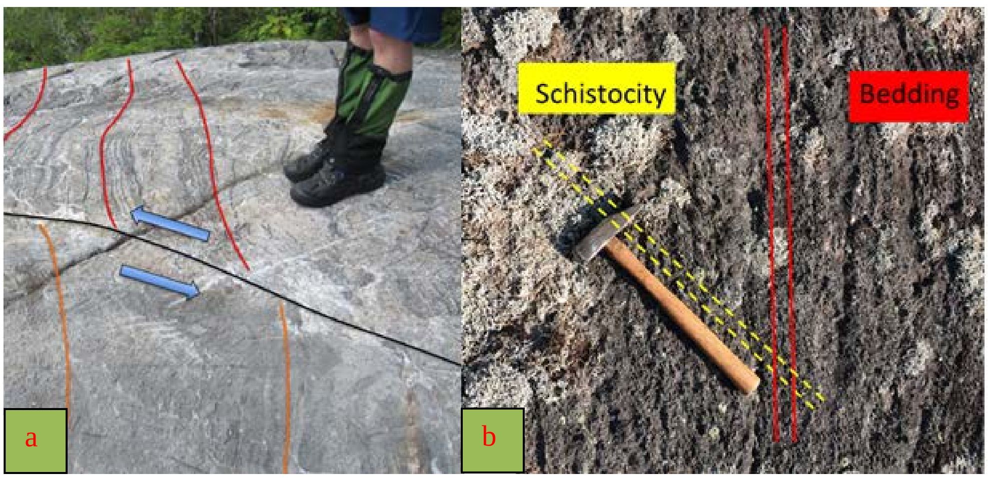

Figure 6. (a) Pre-metamorphic faulting from Eusden, Rankin and Moench talk (2013). (b) Annotated anti-parallel bedding and schistocity from Bog Brook Hill.

Field structures can also provide direct evidence of deformation at different stages. Some features prove to be more challenging to identify than others. Figure 6a shows a migmatized sinstral shear zone. This faulting would have occurred prior to regional migmitization, meaning that it was likely a product of Salinic deformation. 6b shows the anti-parallel relationship of bedding in schistocity. Although bedding and schistocity are parallel in most parts of Acadian folds, at the hinge line of the fold they become anti-parallel. Outcrops such as these are important for showing meso-scale folding that can be directly correlated to the Acadian orogeny.

Metamorphism

The most significant tectonic event in this study area is the Acadian Orogeny, which progressed across the CMB between the late Silurian and base of the Frasnian (Bradley et al, 2000). Bradley et al (2000) place the deformational front of the Acadian Orogeny in the Gilead, Maine 7.5' quadrangle at the base of the Lochkovian (figure 7). These researchers show the progression of the Acadian orogeny, which had moved almost entirely through Maine by the Eifelian, using CZ dates derived from zircons in plutons. Bradley et al (2000) describe two distinct phases of ductile deformation: 1) an establishment of schistocity and early folding in the Acadian foreland basin, and 2) large scale folding during the advance of the Acadian deformational front.

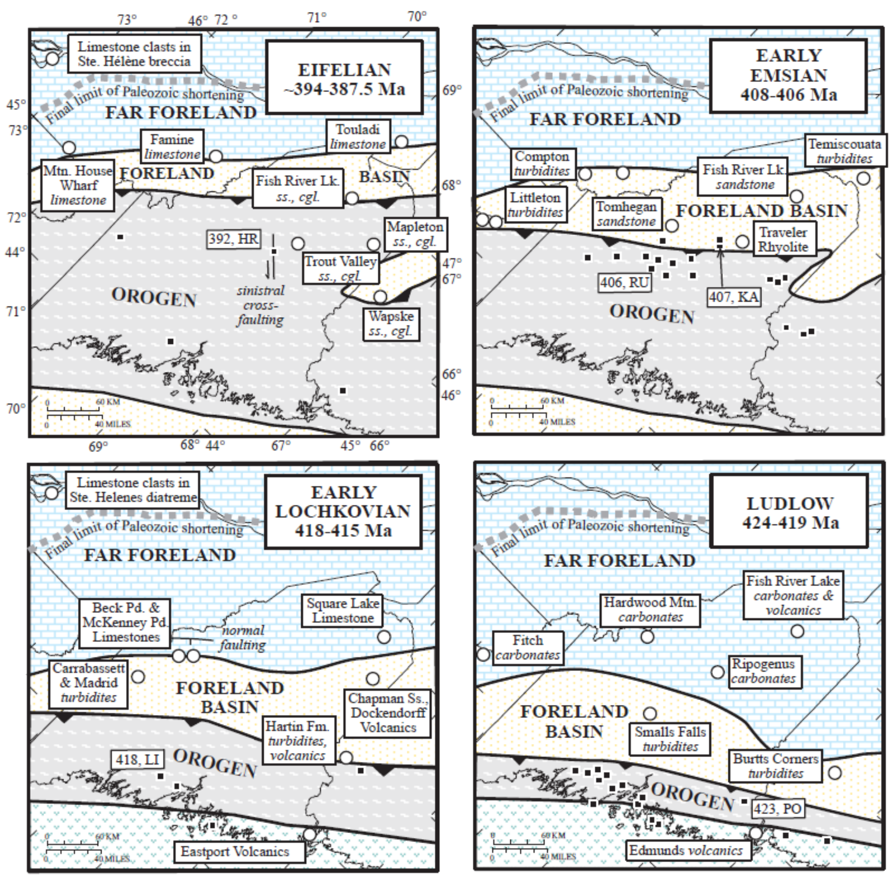

Figure 7. Acadian orogenic progression over Maine with time signatures based on significant dated plutons (Bradley et al, 2000).

During the Acadian orogeny, the strata deposited in the CMB were deformed episodically by fold-thrust nappes with westward vergence, back-folding of early structures, northeast trending upright folds, east to north-west trending upright folds, and north trending upright folds, which has caused complicated interference patterns (Osberg, 1978). For clarity, a correlation chart is provided (table 1). According to De Yoreo et al (1989), in southwestern Maine, the mineral assemblages in the Silurian and Lower Devonian rocks suggest a burial depth of 10-15km. This depth analysis supports the low pressure/high temperature metamorphic character of the Rangeley, Smalls Falls, and Madrid formations. Other rocks from Sebago Lake, northern Coastal Portland, Maine are described by Solar and Tomasack in the 2016 NEIGC Field Guide. These units named the southern Maine migmatite-granite complex (MGC) show high temperature petrogenesis. Solar and Tomasack (2016) have separated the MSC rocks based on their structural history (derived from geochronology and geochemistry) and cross cutting relationship to show that the Sebago pluton is intruding into the older, metasedimentary units.

Additional contact metamorphism caused by the high frequency of intruding plutons is also evident in the study area. Previous studies (Watermulder, 2014; Choe, 2014) found evidence of quartz diorites and granites that have intruded through metasedimentary layers, placing their intrusion during the end of the Acadian Orogeny. Contact metamorphism is responsible for the overwhelming presence of migmatites in the study area.

Orogenic Event	Timing (ma)	Structural Description
Taconic	Middle Ordovician to Upper Ordovician	Fold thrust nappes and recumbent folds with westward vergence
Salinic	Late Silurian	Back folding of early Ordovician western folds
Acadian	Late Silurian to Early Devonian	Northeast trending upright folds
Acadian	Middle Devonian	East to northwest trending upright folds
Acadian	Middle Devonian	North trending upright folds

Table 1. Correlation chart showing structural features described by Osberg (1978) and De Yoreo et al (1989) matched with known regional tectonic events. Data provided by Osberg (1978).

The Acadian orogeny is ubiquitously credited for the metamorphism that can be seen in Western Maine. Evidence of other orogenic events is limited to pre- and post-Acadian analysis of jointing, thrusting, and fracturing that can be attributed to the Silurian, Neoacadian, Alleghenian orogenies.

To reiterate, the primary purposes of this study are as follows: 1) To provide a complete evaluation of regional syn and post-deformational ductile history of New England based on the data gathered in the Gilead, Maine 7.5’ quadrangle. 2) To correlate this deformational history with known orogenic events, such as the Salinic and Acadian orogenies. 3) To correlate igneous and metasedimentary units in the study area with known plutons and stratigraphic formations respectively. 4) To provide an accompanying fold map and cross section to better portray sub-surface structure in conjunction with the bedrock contact map generated by Wheatcroft (2017).

Methods

Field Mapping

Field mapping was completed over four weeks during the 2016 summer field season. Forty hours of fieldwork were logged each week. Fieldwork consisted of traverse planning, execution, and preliminary mapping by hand. The southern Gilead, Maine 7.5’ quadrangle is a heavily forested area, interspersed with logging roads, snowmobile trails and hiking paths, as well as many brooks and streams. The 2016 field season was abnormally dry, creating ideal conditions for outcrop access via rivers and streams. Often, these paths would not coincide with locations of predicted maximum outcrop density, so bushwhacking was common, particularly when accessing steep slopes. Traverses were plotted to encounter areas of highest potential exposed outcrop. These predictions were influenced by three primary factors: 1) knowledge of glacial till accumulation, which obscures bedrock (Thompson et al, 2014), 2) a contour map of the Gilead, Maine 7.5’ quadrangle, on which steep slopes were sought out (Figure 8c), and 3) local advice, particularly when accessing private property.

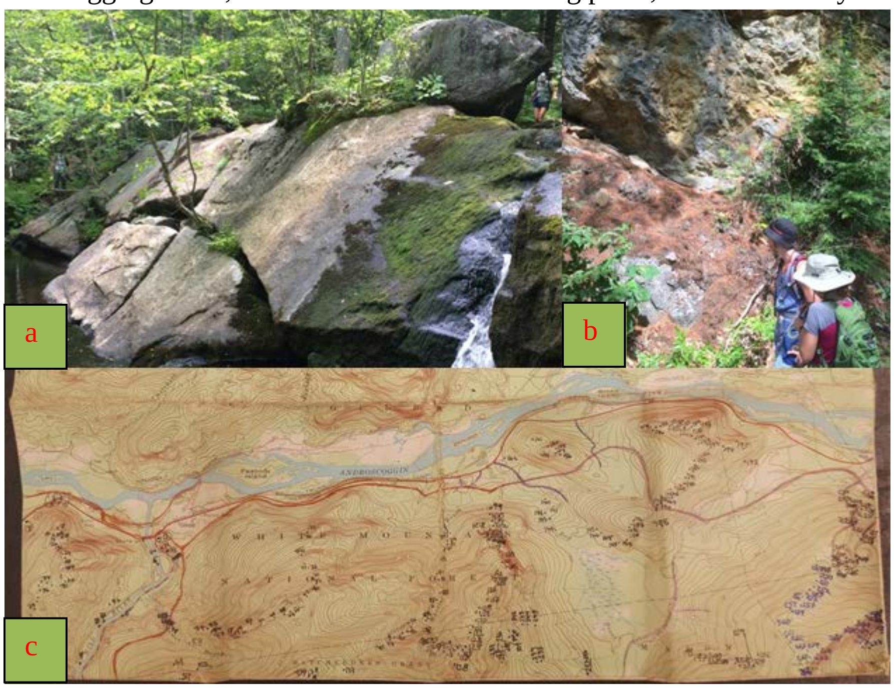

Figure 8. a) Large river outcrop at Bog Brook. b) Roadside exposure located along US Route 2. c) USGS topographic map of the Gilead, Maine 7.5’ quadrangle contour map used to hand plot data points and plan field traverses.

At each outcrop strike and dip data were taken for both bedding and foliation, which were generally parallel. Lithology, stratigraphy, and meso-scale fold data, such as hinge lines (trend and plunge) and axial planes (strike and dip), were also collected when available. Data was measured with a Brunton field compass using the right hand rule, and recorded in a Rite-in-Rain field notebook as well as a Trimble-Juno handheld GPS. Outcrop location and notes were periodically transferred from the Trimble-Juno onto ArcGIS in order to safeguard from data loss and to facilitate subsequent digital mapping.

285 data points were collected during the field season. In regions of dense outcrop exposure, outcrops were recorded at ~50m intervals or when significant compositional changes occurred. On large continuous outcrops, multiple data points were collected. When forest outcrops were obscured due to moss or other vegetation, peels were performed to expose outcrops. Due to the migmitized nature of the

rocks, there was a significant amount of variability in strike and dip measurements of fold axial planes, as well as trend and plunge of hinge lines.

Over 50 hand samples were taken from all significant stratigraphic units using a rock hammer. Key rock types collected included schists (grey and rusty), quartzites, granofels, calc-silicates, two mica granites and pegmatites. The data collected here were used to create fold and contact maps (Wheatcroft, 2017) on ArcGIS with a complimentary 1:1 cross section, and have been used to contribute to an ongoing mapping project for the Maine Geological Survey along with data gathered by Sula Watermulder (2014) and Saebyul Choe (2014) in the 2013 field season, and Dykstra and Riley Eusden (2015) in the 2012 field season.

Thin Section Preparation

Nine hand samples were selected for thin section from those collected during the field season. These hand samples were chosen based on their quality, location, and their representation of all major stratigraphic units that were encountered in the Gilead, Maine 7.5' quadrangle. Samples made into thin section included three granites, two granofels, a quartz diorite, a calc-silicate pod, and two schists (one rusty, one grey). The chosen samples were taken from a wide distribution in order to best represent all significant bedrock units. These hand samples were cut and trimmed using rock saws shown in figure 9.

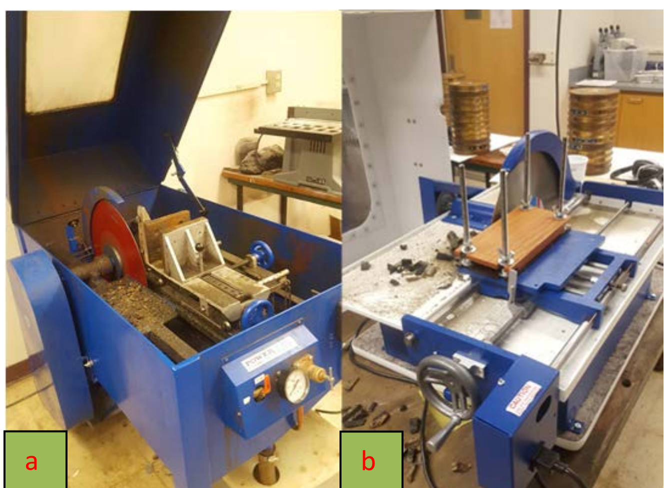

Figure 9. Rock saws for thin section production. a) Diamond Pacific TR-18 Slab Saw, used for initial cutting. b) Lortone, Inc. Lapidary Trim Saw FS8, used to trim cut samples into rectangles.

Samples were cut to expose a ~27x46mm rectangular surface. In foliated rocks (schists, granofels) the samples were cut perpendicular to foliation in order to best show those features in thin section. The nine cut and trimmed samples were sent to Spectrum Petrographics in Vancouver Washington to be mounted and polished. All thin sections were made with a standard thickness of 30μm. Total production time for thin sections at Spectrum Petrographics took three weeks, and thin sections were received in late October, 2016.

Thin Section Analysis

Thin sections can provide a more detailed perspective on regional deformation by revealing the character of foliations at the micro scale, which can help place rocks at certain positions in an orogenic belt (Fossen, 2010). The extent of the effect that strain has had on metamorphism can be shown in thin section through grain size, orientation and recrystallization. Thin sections also allow for a more meticulous analysis of mineral composition, which provides details on provenance and recrystallization during metamorphism, as well as metamorphic grade. Finding the metamorphic grade of rocks through mineral composition can help identify the temperature and depth at which the rocks were formed, and thus further show the location of rocks within an orogenic event. For example, a thin section showing high concentrations of pyroxene, olivine and plagioclase is likely from a granulite, a relatively high-grade metamorphic rock. Minerals like chlorite and actinolite are more commonly found in lower grade metamorphic rocks, such as greenschists (Fossen, 2010).

Thin sections were analyzed with an Olympus BH-2, model BHSP polarizing microscope using transmitted light microscopy (Figure 10). Minerals were photographed through this microscope using an Olympus DP21 camera. Unique mineral properties, such as the twinning of feldspars, were highlighted in cross-polarized light and photographed.

Figure 10. Olympus BH-2 model BHSP polarizing microscope.

Stereonet Generation and Analysis

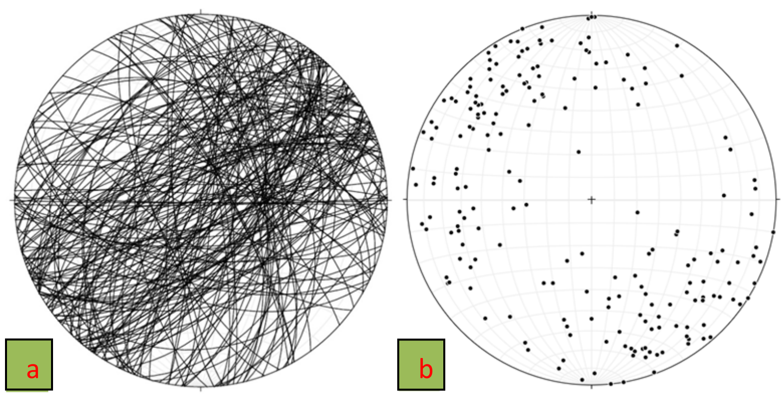

Figure 11. Beta and pi diagrams of planar S_0&S_2 field data, plotted in Allmendinger's Stereonet v.9.8.3. a) Beta diagram of planar data gathered in 2016 field season in Gilead, Maine 7.5' quadrangle. b) Pi diagram of 2016 Gilead, Maine 7.5' quadrangle field data.

Bedding, foliation and fold data were exported from ArcGIS into a Microsoft Excel sheet. Using Allmendinger's Stereonet v.9.8.3, planar data was used to generate a beta diagram, which was converted into a pi diagram for contouring (Figure 11). Beta and pi diagrams are two-dimensional representations of three-dimensional structures, as shown in Figure 12. In beta diagrams, great circles, represented by lines, show the strike and dip of planar structures (using the right hand rule). Pi diagrams show the poles to those planes, which are represented by points. The purpose of plotting the bedding and foliation data together was to reveal any regional folds in the study area. Regional fold character was calculated from the pi diagram of bedding and foliation (S_0&S_2). This pi diagram was contoured using Kamb contouring with one interval of spacing. Single interval spacing versus higher order intervals will expand the range of contour map within the stereonet. With these data, a cylindrical best-fit line was plotted using Bingham Axial distribution. Bingham Axial distribution is used where data are presented as axes rather than lines. It is reliant upon calculating a value referred to as the orientation tensor from the cosines of the angles of individual eigenvalues and eigenvectors to get the principal axes of the tensor. The specific Bingham Axial distribution formulae can be found in the Stereonet 9.5 manual by Allmendinger et al (2012). The pole of the cylindrical best fit line represents the trend and plunge of the hinge line of the axial plane of the fold. The dip of the axial plane was calculated by bisecting the dips of the fold limbs. Smaller folds were also analyzed in Stereonet. Fold data were taken from the field, and were grouped together based on fold generation. These meso-folds were highly migmatized, and may shed light on deformation that occurred simultaneously with partial melting in the rock.

a

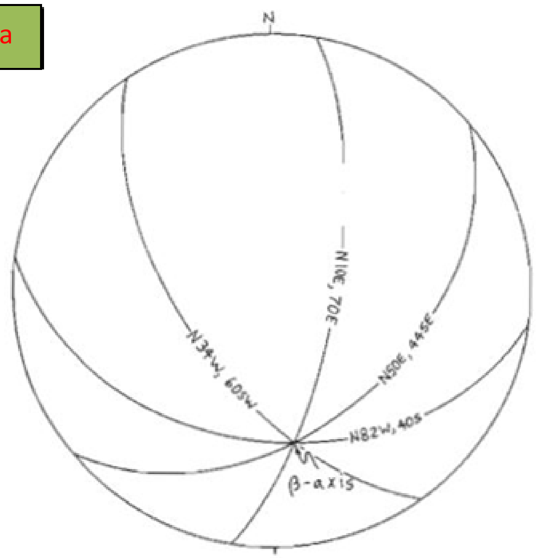

b

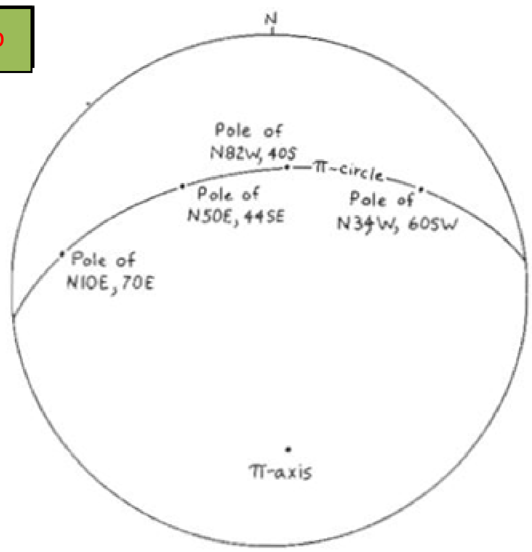

Figure 12. Beta and Pi diagrams are used to interpret fold data.

A) Beta diagrams offer a simple method for determining the axis of a cylindrical fold. Any two planes tangent to a folded surface intersect in a line referred to as the beta axis. The beta axis is the intersection point of the planes.
B) For plotting large numbers of data points, pi diagrams are the preferred method. Pi diagrams consist of the poles of planar beta diagram data. Poles to planes are represented by points, and are 90º to planes. These data can be used for statistical analysis, which can show limbs of major folds. Poles to planes cluster along greater circles, which can be calculated in Allmendinger’s Stereonet v.9.8.3.

Figures provided by Taylor et al, 1997.

Fold Classifications

In order to properly understand the extent of deformation in the Gilead, Maine 7.5' quadrangle, a critical analysis and classification of the folds in the study is required. There is evidence of folding and deformation in the rocks of Gilead at the micro, meso, and macro scale. Using specific tools and analytical techniques, each of these fold types can be better visualized and quantified for this study, and shed light on the character of deformation across the Gilead, Maine 7.5' quadrangle.

The folds that we have found in the study area will be broken into generations, correlating them to a specific deformational event. In this thesis, first generation folds will be referred to as D_2, as D_1 (Salinic) deformation did not cause folding in our study area. Second generation folds are therefore designated as D_3 (Acadian). Any deformation post-dating D_3, such as rifting or faulting, is referred to as a D_4 (Neoacadian or Alleghenian) event.

Micro fold analysis was performed in thin section, using the Olympus BH-2 petrographic microscope. Features such as folded foliations are indicative of D_3. D_2 can also be seen where bedding is antiparallel to foliation. These features are also shown well in meso folds.

Meso scale folds are structures that can be seen and measured at the outcrop level. These types of folds are useful for a few key reasons: 1) meso scale folds still show what generation fold they are by their relationship with foliations and 2) in some cases they can be used to create a domain map, which can be used to view trends in fold direction over the study area. In our study area the meso folds are prone to syncollisional and post collisional migmitization, and therefore have a wide range axial plane strikes and dips. This unfortunately makes them considerably less useful for showing general trends in strike over a large-scale map. For this reason, a domain map is not particularly useful for this thesis.

Figure 13. Outcrop scale fold from 2016 summer field season outlined in red showing bedding and foliation deformation, classifying this as a D_3 fold.

On the macro scale, folds are understood primarily through stereonet analysis, in which limbs are interpreted as the greater circle of the highest density cluster of poles. For this study, as was previously mentioned, all bedding (S_0) and foliation (S_1) data were used to generate these fold maps.

These folds are then quantitatively interpreted based upon the features that have been observed through the previously mentioned methods. Folds can then be classified on a Fleuty diagram (Figure 14a) based on the plunge of the hinge line, and dip of the axial surface. The Fleuty diagram shows the angle that the fold is plunging, and the degree to which it is recumbent.

Folds are also classified by their interlimb angle (Figure 14b). This is simply the angle created between the two limbs of a fold. The degree of the interlimb angle is indicative of the strength of compressive force that created the fold. Smaller interlimb angles reflect more extreme deformation histories. Dip isogons are also key in fold classification (Figure 14c). Dip isogons are constructed by connecting lines between the outer and inner arcs of a fold in order to better understand the unique geometry of a fold. Dip isogons divide folds into three classes (Fossen, 2010): 1) concentric or parallel. Isogons radiate out from the axial plane 2) Similar folds. Isogons are parallel to axial plane, or nearly so 3) Divergent. Dip isogons diverge from the axial plane.

Folds can also be refolded or overprinted upon one another (Figure 14d). This makes for complex fold geometry, but is common, particularly in areas where there are multiple generations of deformational events. Refolded folds can create an array of unique patterns in bedrock, depending entirely upon the relationship of the two or more deformational events that have caused them. Understanding these later generations of folding and their mechanisms is crucial for showing the provenance of deformational events.

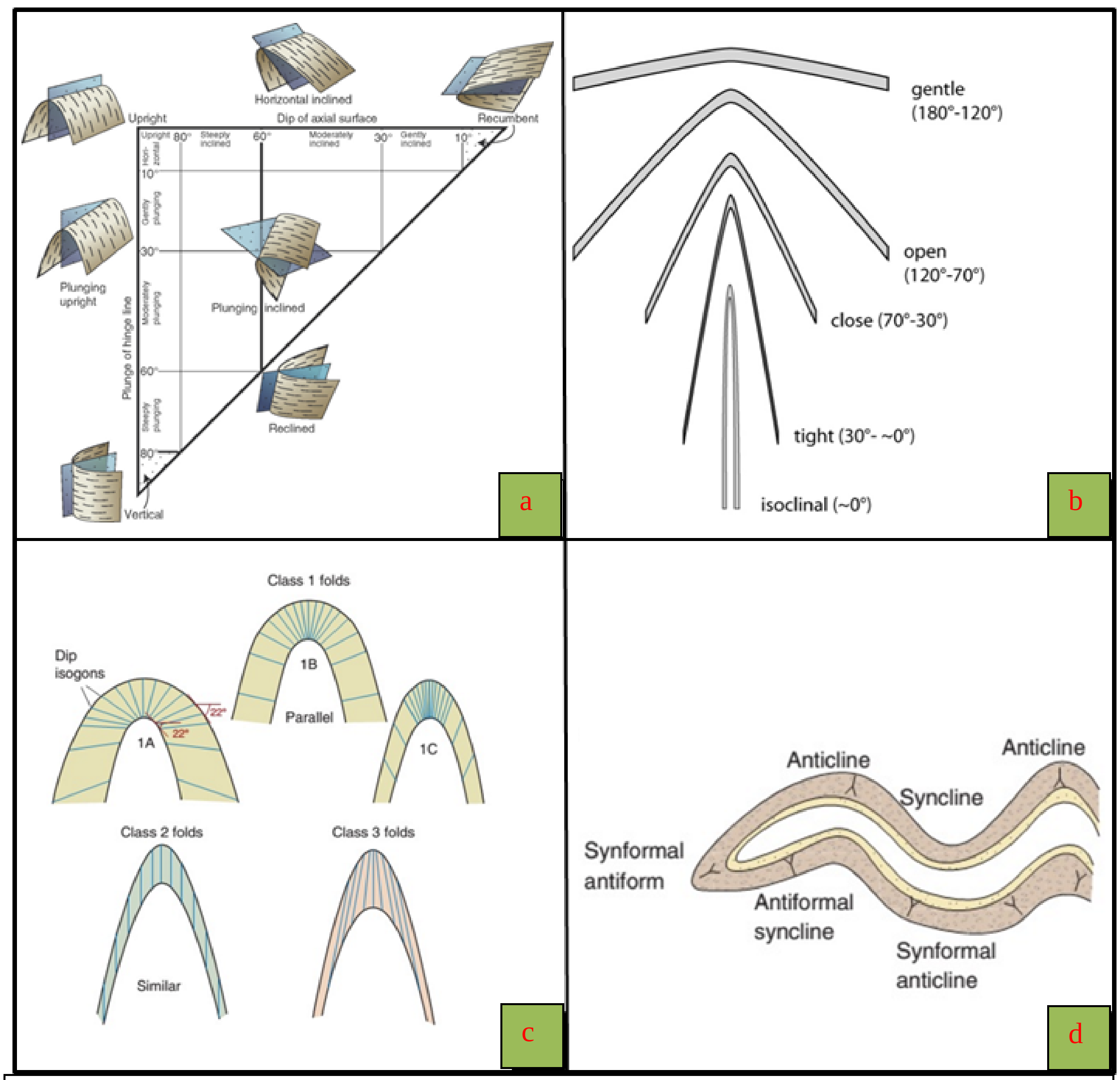

Figure 14. a) Fluety diagram (Fossen, 2010). b) Inerlimmb angle chart (Press and Siever, 2003). c) Fold isogon classes (Fossen, 2010). d) Refolded fold with nomenclature (Fossen, 2010).

Fold classification plays a significant role in comprehending deformational strength and extent, and is therefore the primary focus of this thesis. Folds classified using these methods have been drawn and digitally mapped on an updated bedrock map of the study area using ArcGIS.

Cross Section

Cross sections are visual representations of the subsurface interactions of geological beds. Cross sections are particularly useful when dealing with areas that have a complex folding history, and can be used to effectively show these complicated bedrock relationships. Cross sections vary in length, depth, and strike in order to best represent the bedrock in question.

When constructing a cross section, it is important to have a clear understanding of the nature of folding and structure in the study area. The cross section location is chosen based upon the location of the most interesting and revealing geological features on a contact map. The strike of a cross section is set perpendicular to the axial plane of major folds, in order to best show those features. After selecting a cross sectional strike, subsurface interactions between stratigraphic layers can be sketched. Here, field data becomes quite important. Using strikes and dips of spatially significant outcrops, the dip of layers on cross section can be calculated. This calculation, shown below, yields a value referred to as the apparent dip (d_a).

$$\tan(d_a) = tan(d_t) \times \cos(S_{xs} - T_{dt})$$

Here d_t represents the true dip of the beds, T_{dt} the true strike, and S_{xs} is the dip of the cross section (Visible Geology, 2014).

Cross sections also rely heavily on interpretations of macro scale folds. Using stereonets, the expected dip of each limb on macro folds can be calculated and transcribed onto a cross section, allowing for a realistic depiction of subsurface interactions. These cross sections are crucial for deformational interpretation, particularly in a study area that is as folded and migmatized as the Gilead, Maine 7.5' quadrangle. The cross section in this study is drawn with no vertical exaggeration. An elevation profile from A to A' was found using Google Earth Pro and scaled appropriately.

Geochronology Significance

Although the age of stratigraphic units can be predicted based on the correlation of lithologies to other regions and cross cutting and deformational relationships, this is not definitive proof of the stratigraphic ages. In order to truly establish a timeline for orogenic events that have affected the Gilead, Maine 7.5'quadrangle, an aspect of geochronology must be applied in addition to structural interpretation.

For deformational events occurring during the Silurian and Devonian periods, zircons are an appropriate tool to use for orogenic dating. Key rock samples have been dated using Detrital Zircon (DZ) and Crystallization Zircon (CZ) ages by Audrey Wheatcroft (2017). Analyses were completed at GeoSep Services in Moscow Idaho. The data gathered here show DZ ages for metasedimentary units based on U/Pb ratios (for more in depth information of DZ and CZ dating, observe Bradley and O'Sullivan, 2016). DZ ages on these rocks will provide an age of deposition, which would qualify as the maximum age for the beginning of orogenic deformation. CZ ages of key cross-cutting plutons, selected by location, yield bracketing dates for the deformation fabrics that are cut by plutons. Using DZ and CZ ages in unison allows for the bracketing of deformation timing in the study area between the DZ age (onset of deformation) and CZ age (end of deformation). Using this information, orogenic timing has been compared to previous data gathered by Bradley et al (2000).

Literature

This thesis not only relies on the analysis of data obtained during the 2016 field season, but also on previous studies done in adjacent areas. These publications and maps provide context for results and comparisons for models and interpretations. There is an immense amount of published literature pertaining to the geology in New England, which provides information on what to expect in the field, helps to understand the complex deformational suite in the study area, and enhances general knowledge of the region. Without these publications from both researchers and fellow students, an informed interpretation of the data would not be possible.

Results

This thesis has produced an interpretive cross section (figure 42) complimentary to the bedrock contact map created by Wheatcroft (2017), a structural map (figure 43) based on the contact map, and an analysis of the three generations of deformation bracketed between 435 Ma and 352 Ma (Wheatcroft, 2017). The various folds identified in the area are separated by generation and interpreted sequentially. Thin sections are utilized to show micro-scale deformation. Important mineralogy is noted and used to bolster interpretations of depositional history. These techniques are used in conjunction to match lithologically and structurally unique units in the Gilead, Maine 7.5’ quadrangle with known regional formations.in Maine and New Hampshire.

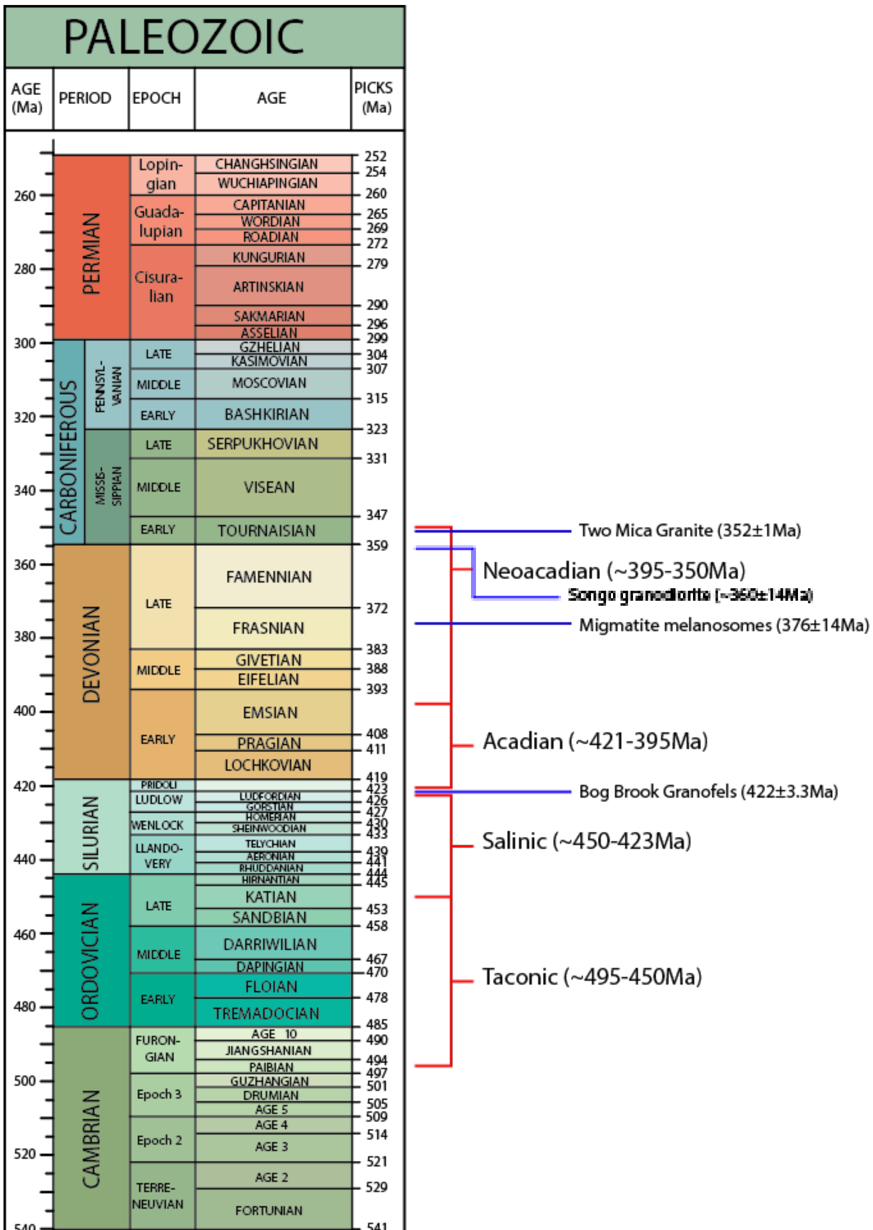

Figure 15. Paleozoic time scale showing age of orogenies based on timing from van Staal (2009) bracketed in red. Blue lines highlight DZ and CZ ages of metasedimentary and igneous units from Gilead, Maine 7.5’ quadrangle (Wheatcroft, 2017; Gibson et al, 2017; Solar and Tomascak, 2016).

Timing of Deformation

Three generations of deformation have been identified in the southern portion of the Gilead, Maine, 7.5’ quadrangle. These periods of deformation have been correlated to the Salinic, Acadian, and Neoacadian orogonies, and will be referred to as D_1, D_2, and D_3 deformation respectively. The majority of D_1, and to a lesser extent D_2 deformation, is obscured within the study area due to orogenic overprinting. Because of this, there is only one location within the study area that shows folding attributed to by D_2 deformation, and there is no exposed outcrop evidence of D_1 deformation. The nearest outcrop example of D_1 deformation was found in the northern half of the Gilead, Maine 7.5’ quadrangle in the 2013 field season by Sula Watermulder (2014), Saebyul Choe (2014) and Dykstra Eusden (Figure 6a).

The timing of these events is shown in Figure 15. This timing is constrained by DZ ages from the Bog Brook Granofels unit, a fine-grained quartzose metasedimentary turbidite and CZ ages of two separate two mica granites from the Wheeler Mine quarry. These ages bracket the timing of the Latest Salinic, Acadian and Neoacadian orogonies as designated by van Staal (2009).

Salinic Deformation (D_1)

There is little evidence of Silurian deformation within the Gilead, Maine 7.5’ quadrangle. Many of the Salinic derived features theorized to exist within the study area have been overprinted by subsequent Acadian and Neoacadian deformation. A single outcrop of Silurian deformation was identified in the Northern Half of the Gilead, Maine 7.5’ quadrangle in the 2013 field season (figure 6a) which shows a bedding shift overprinted by migmitization. There was no evidence of Salinic derived folding within the study area.

Acadian Folding (D_2)

D_3 macro scale folds were interpreted using stereonet analysis of the entirety of bedding (S_0) and schistocity (S_2) data from outcrops. Schistocity is referred to as S_2 because it correlates with Acadian D_2 deformation. The combination of bedding and foliation data, which are overwhelmingly parallel within this study area, shows the character of the major antiforms and synforms in the Gilead, Maine 7.5’ quadrangle. Figure 16 shows a contour diagram of the poles to the aforementioned planar data.

As expected, the Acadian schistocity runs parallel with the axial plane of the D_2 folds within the hinge of the fold. In all other areas, S_0 parallels S_2. This pattern suggests that there is isoclinal nappe-scale folding of D_2 age. This same isoclinal folding can be seen in cross sections of exposures at Bald Head, Maine in the Kittery formation (Hussey, 1989).

The potential facing directions of these D_2 fold hinges within the map scale refolded fold system depends on the vergence of the fold system and whether the strata of the southern Gilead, Maine 7.5’ quadrangle comprise the upright or overturned limb of the fold system.

The first D_2 meso scale fold (Figure 16) was located at the northern peak of Bog Brook Hill, within the Bog Brook Unit, a migmitized gray schist (for full descriptions of stratigraphic units, see Wheatcroft, 2017). The strike and dip of the axial plain are 144^o, 86^o and the trend and plunge of the hinge line are 319^o, 52^o. In the D_2 folds (F_2), foliation (S_2) is shown by the yellow dashed lines. S_2 defines the axial planar fabric, and bedding (S_0), highlighted by the solid red line is folded. This fold was found to be open, with a wavelength of 46cm.

The second D_2 fold (Figure 17) was located on Peaked Hill, within the Peaked Hill Unit. This was the only other outcrop location where D_2 folding was visible. S_2 axial planar fabric runs parallel to the shaft of the rock hammer, with folded (S_0) bedding crossing at the hinge of the fold, shown in red. This fold, like that shown in Figure 17, is open with a strike and dip of 247^o, 79^o and a hinge line trend and plunge of 78^o, 44^o.

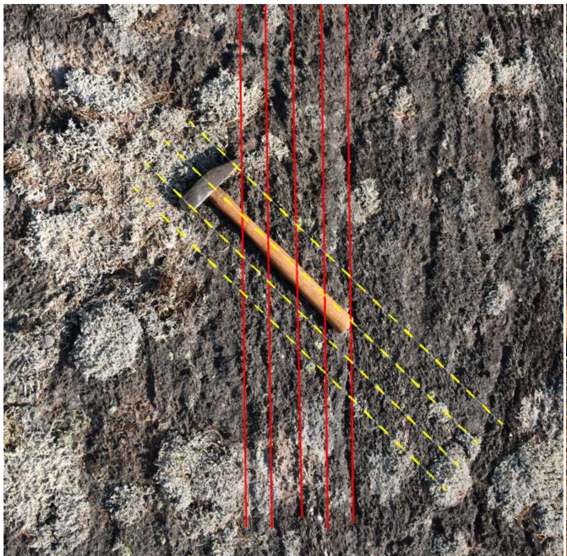

Figure 16. Field station 108, Bog Brook. Hand for scale.

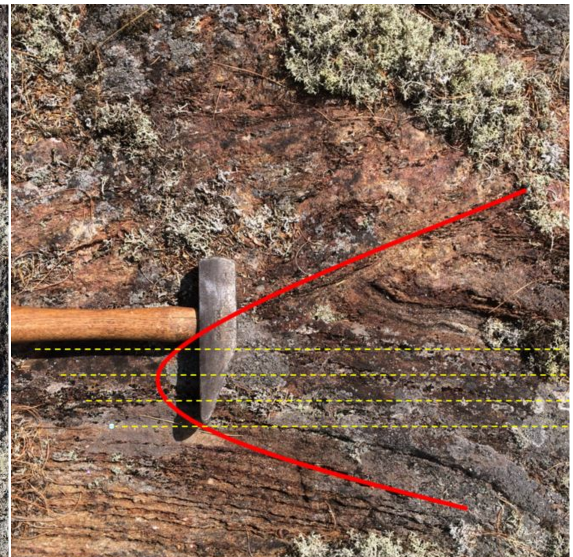

Figure 17. Field Station 128, Peaked Hill unit. Rock hammer for scale.

Figure 18. Bog Brook non migmitized grey schist showing strong foliation of biotites and chlorites (yellow dashed line). Thin section dimensions 27x46mm.

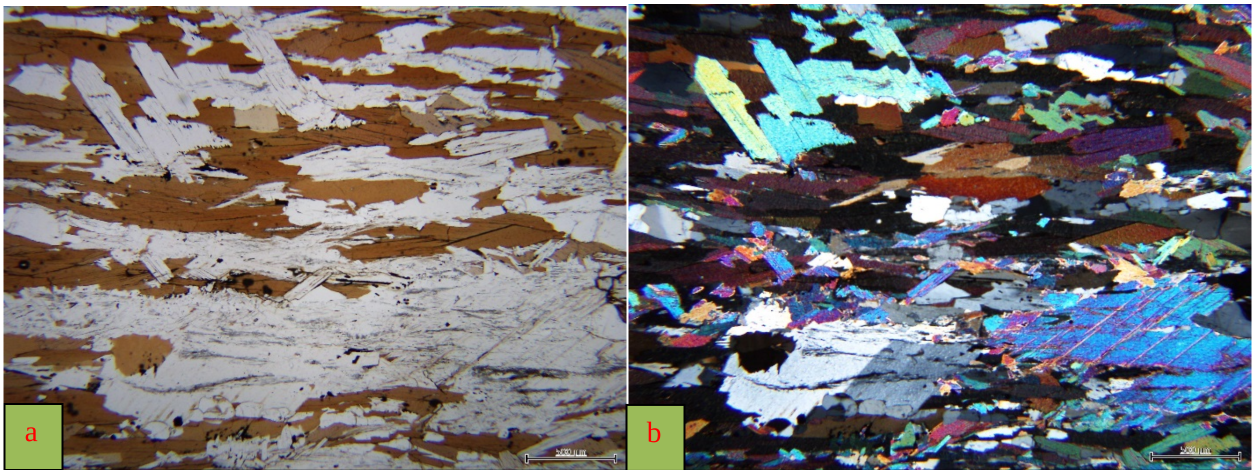

Figure 19. (a) Bog Brook grey schist in plain polarized light. Strong foliation shown by biotite and muscovite alignment. (b) Sample 158 in cross polarized light. Scale bar reads 500μm.

The fabric shown in Figure 18 shows an S_2 foliation formed by alignment of biotite crystals within an unmigmatized grey schist. That same cross section, shown in plain and cross-polarized lighting in Figure 19 contains large grained misaligned muscovite crystals. These muscovite crystals are the product of later stage growth due to high temperature-low pressure metamorphism. This sample contains a high percentage of sillimanite grade metamorphic minerals, including quartz, potassium feldspar, plagioclase, muscovite and biotite, with some transitions to chlorite (Figures 18 and 19). There are also garnets present in small quantities.

Neoacadian Folding (D_3)

There were twenty D_3 generation folds (F_3) found throughout the study area within units that showed a folded S_2 fabric. In these areas, bedding and schistocity ran parallel throughout and both were folded by D_3 deformation. Although F_3 folds were much more common within the study area, they were still affected by post collisional migmitization, which skewed the strike and dip and trend and plunge data, thus muffling any noticeable trends in stereonet. This variable orientation is characteristic of folding that occurred syn-post the formation of stromatic migmatite structures (Solar and Tomascak, 2016).

The F_3 folds here are unique from the F_2 folds in that they have no associated axial planar cleavage. Due to the presence of parallel-layered leucosomes and melanosomes within the host rock, it is unlikely that the metamorphic conditions would have allowed an S_3 cleavage to form.

Two great circles in the stereonet show the fold limbs, which cross near the calculated hinge line (red dot, figure 20) using a cylindrical best algorithm. The limbs of the antiform were found to have a strike and dip of 245^o, 87^o and 345^o, 62^o with a calculated interlimb angle of 83^o. These values were used to accurately depict the antiform and synform in the interpretive cross section. The axial plane of the antiform had a calculated strike and dip of 245^o, 75^o. This calculated value is extremely close to the strike and dip of the S_2 schistocity measured at the hinge line of a D_2 fold in the study area (247^o, 79^o).

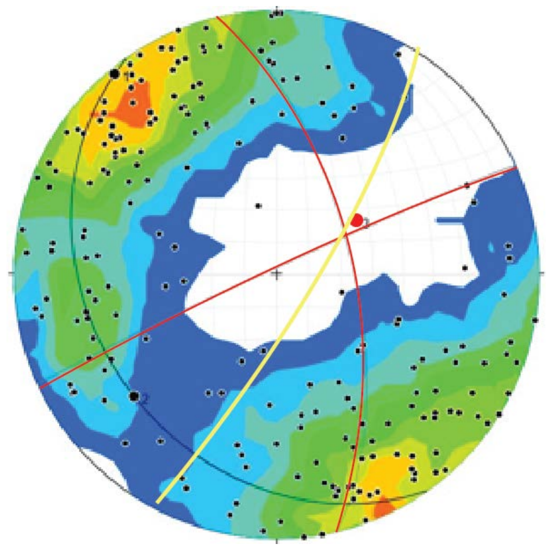

Figure 20. Contoured bedding (S0) and foliation (S2) data from all field sites. Fold limbs (red) dip steeply and strike North and East with interlimb angle of 83 degrees. Axial plane (yellow) dips at 75 degrees. Fold axis (red dot) trend and plunge is 55, 60 degrees.

Figure 21. Field station 1, migmitized grey schist and granofels. Chapman Hill Unit. Red lines highlight bedding, yellow show S_2 cleavage.

Figure 22. Field station 7, migmitized gray schist (xenolith?). Bog Brook Unit.

Figure 23. Field station 8, migmitized grey schist, some calc-silicate pods. Bog Brook Unit.

Figure 24. Field station 10, migmitized rusty schist. Bog Brook Unit.

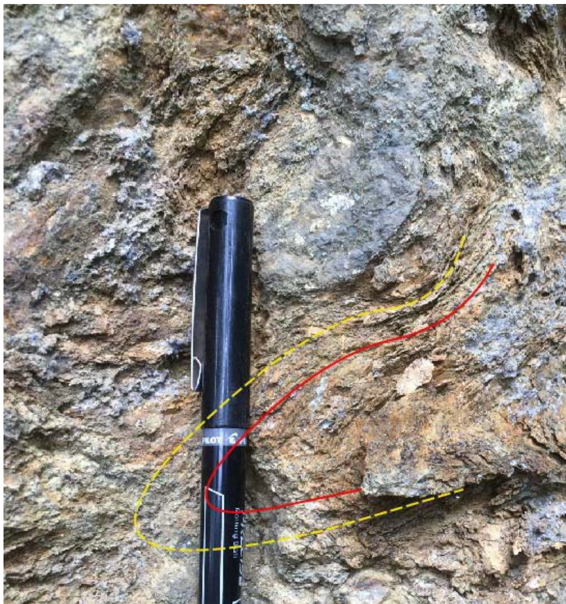

Figure 25. Field station 12, migmitized grey schist with calc-silicate pods and granofels. Peaked Hill Unit.

Figure 26. Field station 13, migmitized rusty schist. Peaked Hill Unit.

Figure 27. Field station 14, migmitized gray schist with parallel leucosome-melanosome layering. Chapman Hill Unit.

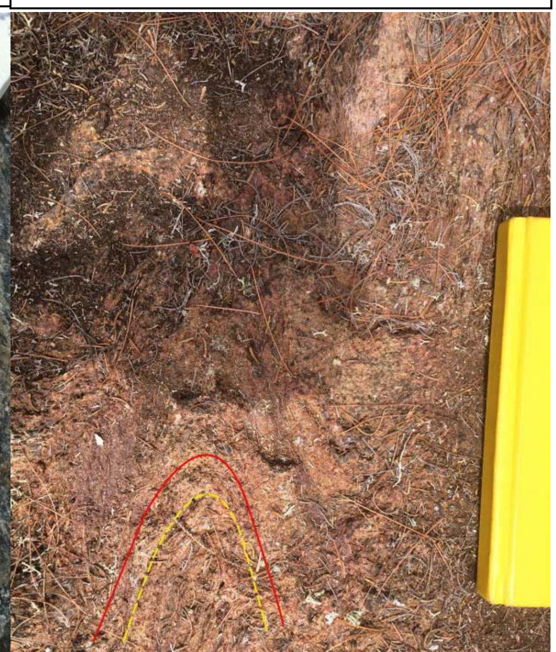

Figure 28. Field station 34, migmitized rusty schist. Peaked Hill Unit.

Figure 29. Field station 73, migmitized gray schist with parallel leucosome-melanosome layering. Bog Brook Unit.

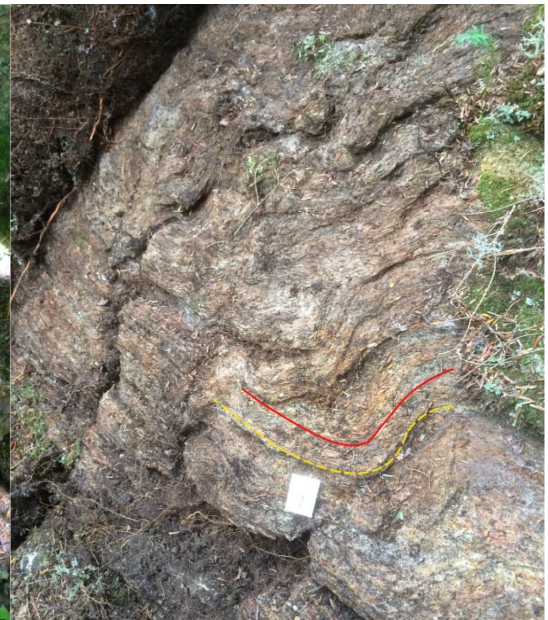

Figure 30. Field station 75, migmitized grey schist. Bog Brook Unit.

Figure 31. Field station 89, migmitized rusty schist. Pine Mountain Unit.

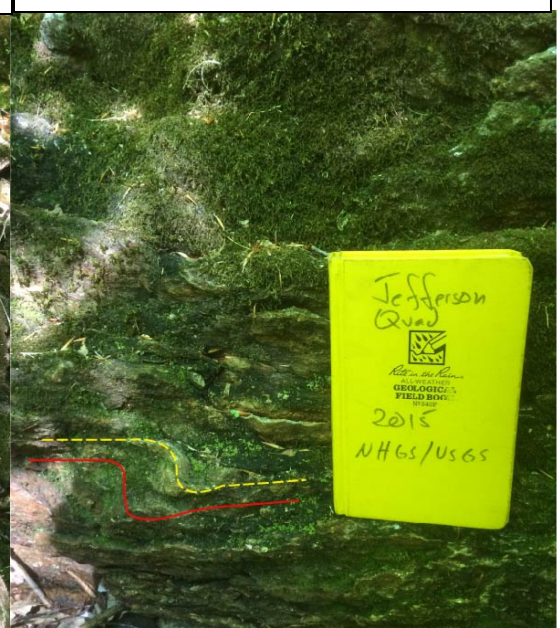

Figure 32. Field station 90, migmitized rusty schist. Pine Mountain Unit.

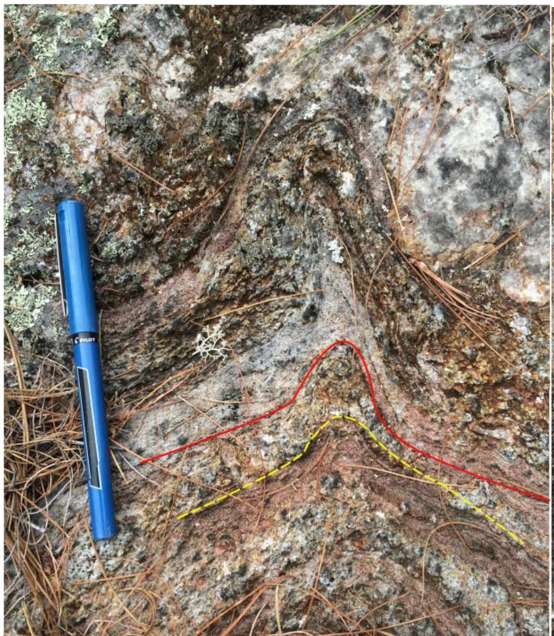

Figure 33. Field station 180, migmitized rusty schist with interbedded aplite. Peaked Hill Unit.

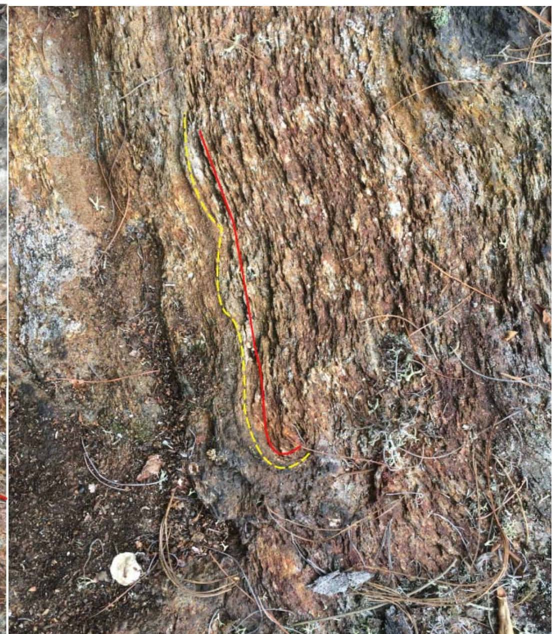

Figure 34. Field station 181, migmitized rusty schist with interbedded aplite. Peaked Hill Unit.

Figure 35. Field station 185, migmitized slightly rusty schist with cm scale crenulations. Peaked Hill Unit.

Figure 36. Field station 190, migmitized slightly rusty schist with interbedded quartzite. Peaked Hill Unit.

Figure 37. Field station 212, highly migmitized grey schist with interbedded granofels. Bog Brook Granofels Unit.

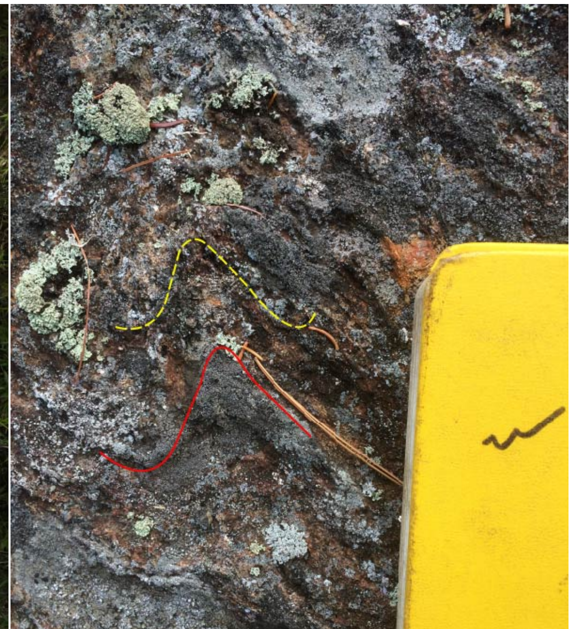

Figure 38. Field station 264, migmitized grey schist (xenolith?). Bog Brook Unit.

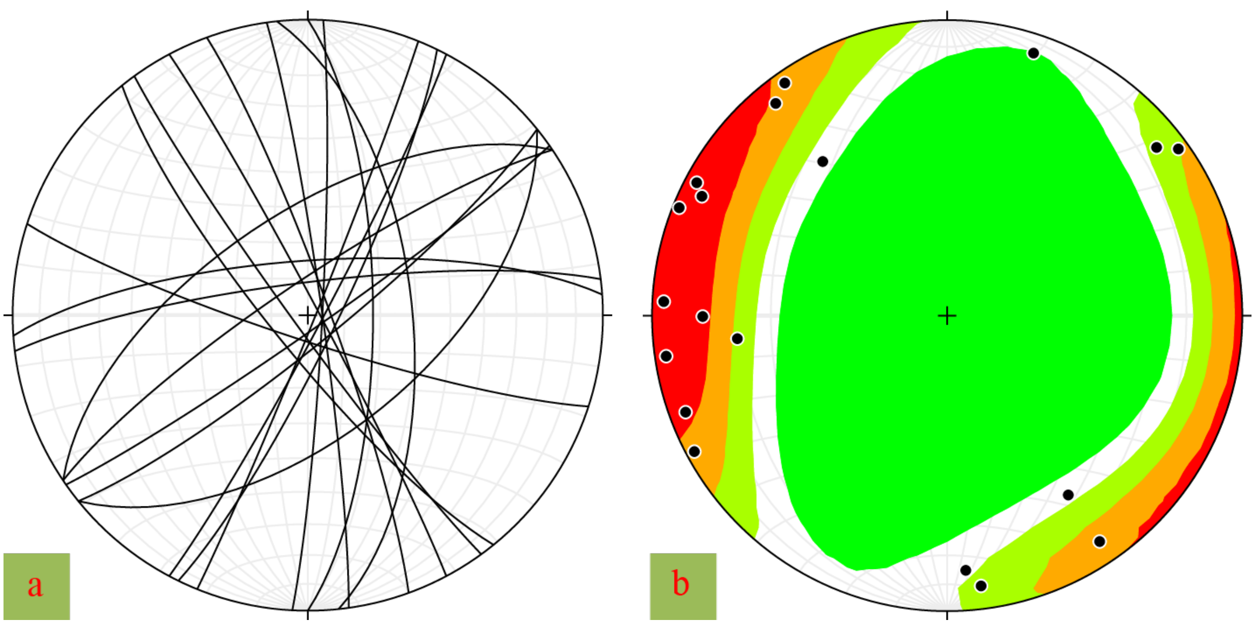

Figure 39. a) Equal area projections of axial planes as great circles and hinge lines as points for all D_3 folds in the study area.

b) Contour map of poles to planes from D_3 axial planes using smoothed Kamb contouring. Plots generated with Allmendinger's Stereonet v.9.8.3.

FoldAxial Plane strike	FoldAxial Plane dip	Fold Hinge Line trend	Fold Hinge Line Plunge
308	74	132	38
332	87	339	56
340	84	344	53
28	86	26	53
296	32	91	20
51	82	47	68
352	86	168	62
3	86	15	66
236	81	80	58
354	61	338	32
51	57	40	22
200	52	205	58
263	81	258	43
55	86	62	50
26	82	212	63
141	80	135	53
108	83	102	78
236	62	259	41
266	75	266	74
0	72	359	54

Avg Dip: 74

Avg Plunge: 52

Table 2. Axial Plane strike and dip and hinge line trend and plunge values for all D_3 folds found in the Gilead, Maine 7.5' quadrangle with average values.

The stereonet made from the available D_3 fold data (Figure 39) does not show an overwhelming trend in strike. A contour diagram of D_3 planes to poles (Figure 39b) shows no significant alignment of poles to axial planes throughout the study area for D_3 folds. The lack of strong fabric correlation is in part due to the limited F_3 fold data available. This serves to underscore the disruptive effect high temperature ductile

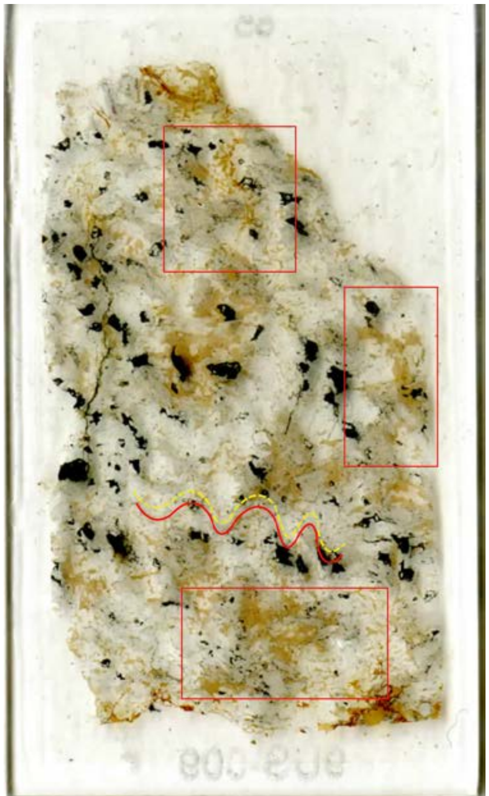

Figure 40. Peaked Hill rusty schist. Red boxes highlight regions of serocite/muscovite alteration. Thin section dimensions 27x46mm.

folding, as evidenced previously from parallel layering of migmatized stromatic structures within F_3 folds.

D_3 micro scale deformation is observed, and shows the interactions of foliations with bedding. In cases where partial melting is more extensive, the leucosome-melanosome relationship is shown by alterations to serocite layers as well as the formation of microscale crenulations.

The Peaked Hill rusty schist (Figure 40) comes from a schist in the rusty Pine Mountain Unit, and as a result presents a much more sulphur rich mineral assemblage. Like the Bog Brook grey schist, the Peaked Hill rusty schist contains a high percentage of sillimanite grade metamorphic minerals, including quartz, potassium feldspar, plagioclase, muscovite and biotite, with some transitions to chlorite. It also contains a higher percentage of grossular than the Bog Brook schist. Serocite appears to be filling in the gaps between the primary micas and silicates. Both samples contain zircons, which appear in biotites surrounded by black "halos" which are the product of radioactive decay.

Within this thin section there are large muscovite crystals that appear to crosscut S_2 foliations and F_3 folding (Figures 40 and 41). The random orientations of these muscovite crystals suggests that they are a product of contact metamorphism that would have had to occur post D_3 activity, and likely correspond with the intrusion of S-type granites within the study area, dated at 352±1Ma. Samples of the Songo granodiorite were dated in a recent study, and were found to be 364±1.3Ma (Gibson et al, 2017). This intrusive unit postdates the ages of local migmatized units from Solar and Tomascak (2016).

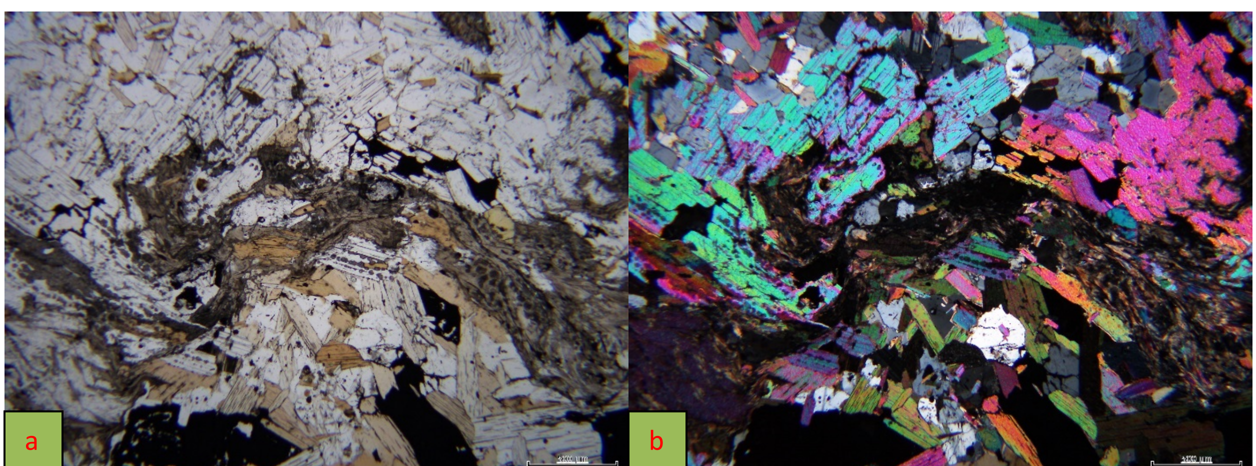

Figure 41. (a) Peaked Hill rusty schist in plain polarized light. F_3 shown by large folded muscovite crystals. (b) Sample 85 in cross polarized light. Scale bar reads 500μm.

Crenulations

At the outcrop and micro scale, crenulations were identified within units affected by partial melting. These crenulations have no associated axial planar fabric. The lack of an associated fabric within these rocks is a byproduct of late D_3 high temperature development of migmatized structures, which caused these units to fold ductily (Solar and Tomascak, 2016). Crenulations range from 5mm to 2cm and can be seen well within folded serocite crystals (Figure 39).

Cross Section

The regional cross section (Figure 42) shows no vertical exaggeration and covers a horizontal distance of 3.50mi (5.63km), passing through every metasedimentary unit in the study area. The map scale antiforms and synforms are the product of initial Acadian folding and subsequent Neoacadian refolding. It is important to note that there are no topping indicators, such as graded beds, within the study area, making it difficult to know if the Bog Brook antiform and Peaked Hill synform are on the upright or overturned limb of the refolded fold.

Structural Map

This structural map (Figure 43), superimposed upon the southern Gilead, Maine 7.5' quadrangle bedrock contact map created by Wheatcroft (2017) shows every meso scale fold plotted with axial plane strike and dip and hinge line trend and plunge. Orientation for D_3 folds is skewed by syn-orogenic migmatic structures, causing large variation in regional strike of F_3 trend.

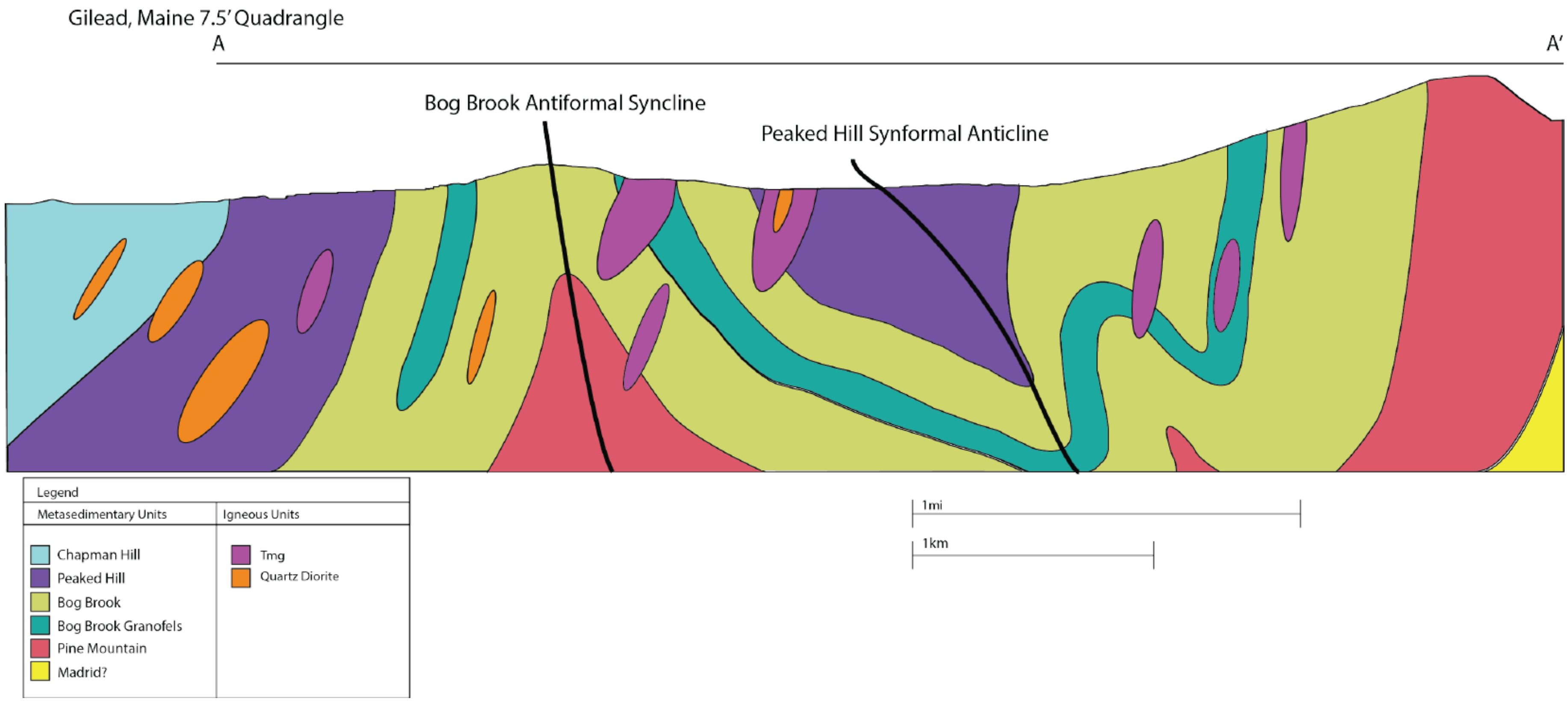

Figure 42. Cross section showing Wheeler Brook antiformal syncline and synformal anticline. Bog Brook granofels (teal) are interpreted to be a discontinuous lens within the Bog Brook Unit. Igneous units are shown intruding parallel to west verging limb of antiform. Subsurface interactions are drawn with no vertical exaggeration.

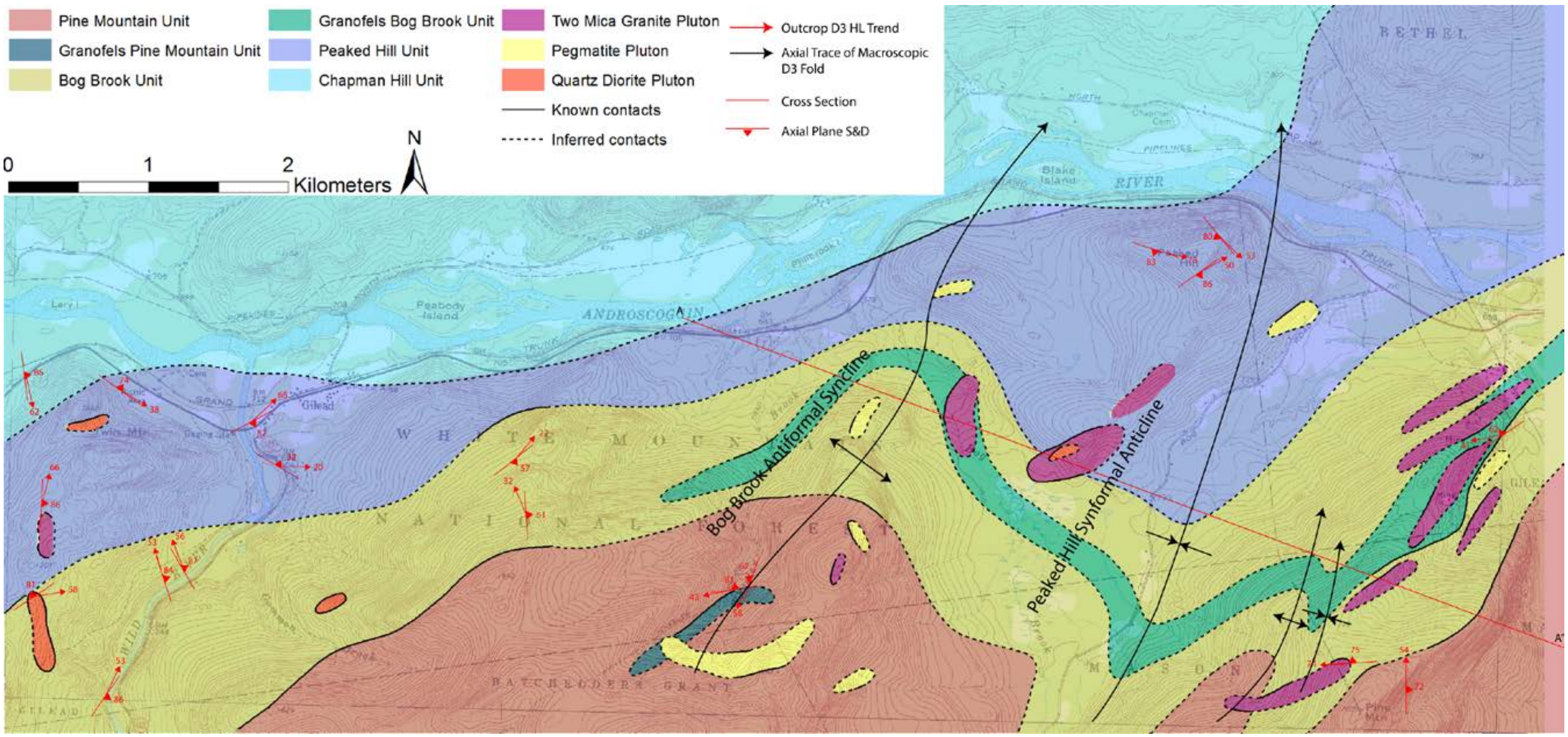

Figure 43. Structural map superimposed upon Gilead, Maine 7.5’ quadrangle bedrock contact map (Wheatcroft, 2017). D_3 folds with associated hinge lines are shown in red. Map scale synform and synform axial traces are designated by black arrows.

Discussion

Local Stratigraphic Correlations

Previous studies in the northern part of the Quadrangle (Choe, 2014; Watermulder, 2014) have reinterpreted the local stratigraphy to show a much stronger presence of the Rangeley Formation in a region that was previously assumed to be a dominated by the Littleton Formation (Moench, 1970). Further stratigraphic analysis in the southern half of the Gilead, Maine 7.5' quadrangle has shown the presence of Rangeley and Smalls Falls formations. The Bog Brook granofels dated by Wheatcroft (2017) show a DZ maximum depositional age of 422±3.3Ma, which correlates well with the expected DZ range of the Rangeley Formation, as shown by Bradley and O'Sullivan (2016). This age also brackets the onset of Acadian deformation within the study area. The area designated as the Pine Mountain unit in this study area has been correlated with the Smalls Falls Formation, the youngest inboard-derived metasedimentary unit of the Rangeley stratigraphy (Bradley and O'Sullivan, 2016).

In the northern half of the Gilead, Maine 7.5' quadrangle, the Rangeley Formation was remapped to occupy the majority of the southern part of the quadrangle, topped by the Perry Mountain, Smalls Falls, and then Madrid formations in that order (figure 44). The order of these stratigraphic units offers clues to the overall structure of the D_2 and D_3 folds that are identified in the Gilead, Maine 7.5' quadrangle and adjacent study areas.

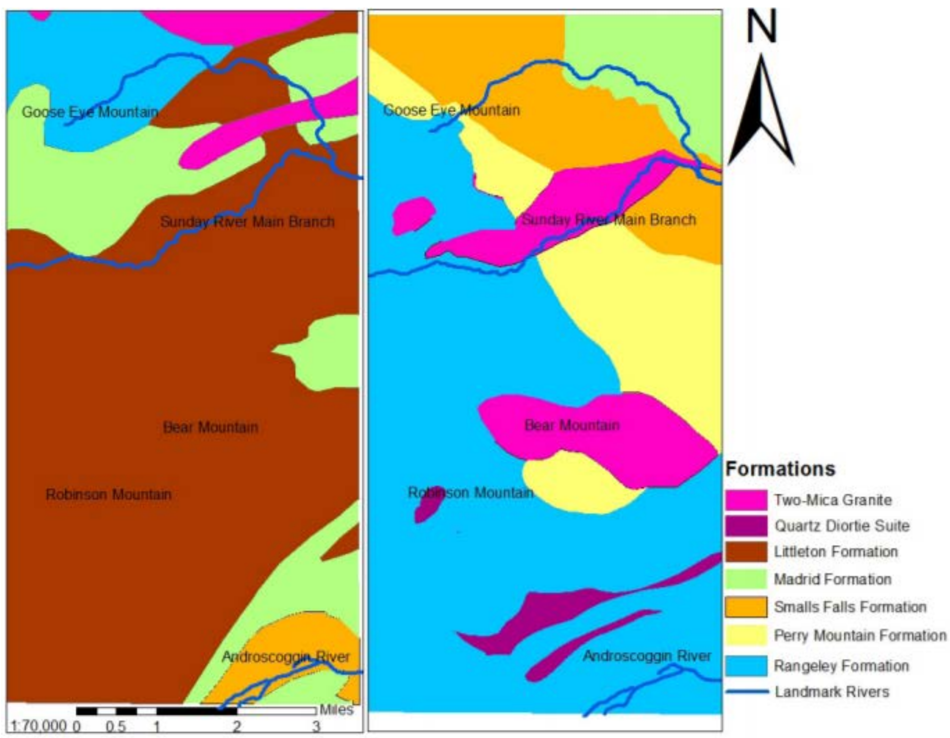

Figure 44. Map view of stratigraphic revisions of data from Osberg et al (1985) to the Gilead, Maine 7.5' quadrangle by Watermulder (2014).

With only the stratigraphy of the northern half of the quadrangle, it is possible to see the effects of Neoacadian refolding on a larger scale. The Rangeley and younger Smalls Falls formations are critical to this observation. In the Northern half of the quadrangle, the older Rangeley Formation rests below the Smalls Falls Formation, however in the Southern half of the Gilead, Maine 7.5' quadrangle there is an inversion in younging direction, and the Smalls Falls Formation lies beneath the Rangeley.

Local Structural Correlations

The structural data available from adjacent study areas have helped to shape the interpretations of the structural data gathered from the southern half of the Gilead, Maine 7.5' quadrangle in this study. Within the study area, the largest andtiform and synform are designated the Bog Brook antiformal syncline and the Peaked Hill synformal anticline. Billings and Billings (1975) identified Silurian-Devonian rocks on the northwest portion of the Gorham, New Hampshire 7.5' quadrangle. The major syncline within the Gorham, New Hampshire 7.5' quadrangle, referred to as the Mahoosuc Syncline, has only 5000ft of Silurian-Devonian strata on its northwestern limb, whereas the southern limb has tens of thousands of feet of Silurian-Devonian strata (Billings and Billings, 1975). This imbalance in Gander cover rock suggests that the depositional basin for the local Rangeley stratigraphy may have been deeper on the southeastern side, before the stratigraphy was inverted due to multiple deformational events.

Salinic Deformation

The first stage of deformation identified in the rocks of the Gilead, Maine 7.5' quadrangle is correlated with the Salinic orogeny in the Silurian. The effects of the Salinic orogeny are cryptic within the study area, and are heavily overprinted by later stages of folding. The only outcrop evidence of Salinic deformation found within the Gilead Maine 7.5' quadrangle was discovered in the northern half of the quadrangle by Sula Watermulder (2014) Saebyul Choe (2014) and Dykstra Eusden in the 2013 summer field season (figure 6a). The offset of the bedding plains is due to faulting that occurred prior to migmatization and refolding events, but remains visible. The bedding offset shown in Figure 45 is the product of a high angle reverse fault that occurred syndepositionally to the Rangeley formation. Retroarc faulting within the Silurian metasedimentary units is the only current evidence of Salinic deformation within the Gilead, Maine 7.5' quadrangle.

Acadian Deformation

The second phase of deformation was initiated in the study area during the onset of the Devonian. The depositional age of the Bog Brook granofels, which have been correlated with the Rangeley Formation, has been dated at 422±3.3Ma (Wheatcroft, 2017). Acadian orogenesis postdates the deposition of units syndepositionally deformed by the Salinic orogeny. Therefore, this DZ date represents the earliest possible time at which the Acadian orogeny would have affected the Rangeley stratigraphy within the Gilead, Maine 7.5' quadrangle.

The D_2 isoclinal folds within the study area are similar to isoclinal folds described by Billings and Billings (1975) within the Jefferson Dome, a unit comprised of a foliated oligocase-andesine with quartz and biotite, and the Ammonoosuc Volcanics, an amphibolite with areas of fine-grained biotite gneiss (Billings and Billings, 1975). These units are located in the adjacent Gorham, Maine 7.5' quadrangle. Similar to the Bog Brook antiformal syncline, the southeast dipping limb of the Jefferson Dome isoclinal folds are overturned. The Acadian orogeny is the first major folding event recognized within the Gilead, Maine 7.5' quadranlge, forming a series of isoclinal folds like those in the adjacent Gorham, Maine 7.5' quadrangle. The vergence of these folds is indeterminate. Similar deformation was also found within parts of the Littleton Formation. The phases of deformation identified within the Littleton Formation are likely bracketed by the same timing constraints used to constrain deformation within the Rangeley stratigraphy located within the Gilead, Maine 7.5' quadrangle.

Outcrop scale Acadian folds were only identified on Bog Brook Hill within the study area (Figures 17 and 18). These folds were identified as Acadian folds based on the antiparallel relationship between the bedding and schistocity. These features are only visible within the unmigmatized regions of the study area, and likely represent the hinge of a minor D_2 fold.

Neoacadian Deformation

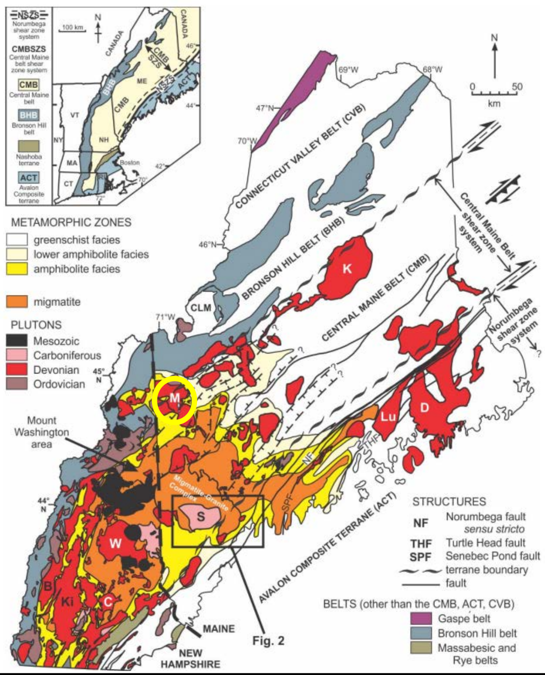

Figure 45. Study area map showing locations of intrusive units throughout Maine (Solar and Tomascak, 2016). Mooselookmeguntic Pluton is shown at location M (yellow circle).

The final phase of folding identified within the Gilead Maine, 7.5' quadrangle correlates with the Neoacadian orogeny. Neoacadian folds were identified at the outcrop scale throughout the study area, and were defined as regions where bedding was folded in parallel with schistocity (Figures 21-38). The Neoacadian refolding phase began immediately after the magmatic conclusion of the Acadian orogeny at the tail end of the Frasnian. The accretion of Meguma to composite Laurentia overprinted Acadian folding in the Rangeley stratigraphy, and formed many refolded fold structures throughout New England. Graded beds on Mount Washington (Eusden et al, 1996) effectively point out the vergence of these refolded fold structures as Eastward.

Neoacadian deformation is bracketed by a CZ age of 376±14Ma from a migmatite melanosome within the Mooselookmeguntic Pluton in western Maine (Figure 45), and is the best current estimate for age of migmatite formation near the study area (Tomascak and Solar, 2016). This age correlates with the intrusion of post orogenic plutons in the study area, which initiated contact metamorphism within the metasedimentary units, causing the ubiquitous migmatization and pegmatite presence within the quadrangle. Solar and Tomascak (2016) speculate that the crustal melting and formation of S-type granites within the Mooselookmeguntic igneous complex may be derived from magmas associated with the Bronson Hill belt crust. This magmatic activity was attributed to by latent flat slab subduction during the welding of Avalon to composite Laurentia (Bradley et al, 2000). The shallowly subduction oceanic crust beneath the CMB initiated an intrusive phase at the end of the Acadian orogeny. This may have been compounded by slab breakoff (van Staal, 2009).

The end of the Neoacadian phase of deformation is bracketed by a CZ age from two S-type granite from the Gilead, Maine 7.5' quadrangle (Wheatcroft, 2017). These granites were found to have a mean age of 351.7±2.1Ma. The intrusion of these granites is associated with further contact metamorphism of metasedimentary units.

Regional Refolding Evidence

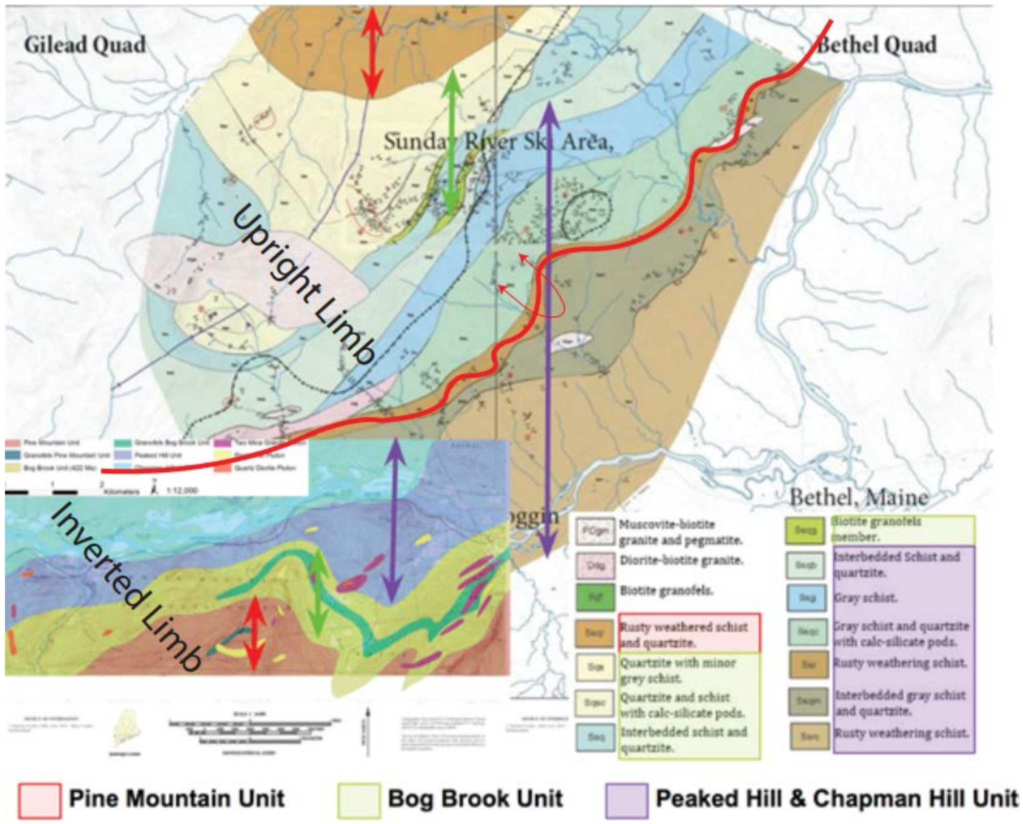

Figure 46. Bedrock maps of Gilead Maine 7.5’ quadrangle and Bethel, Maine 7.5’ quadrangle. Map units are correlated with the unit nomenclature utilized in this study. Figure adapted from Wheatcroft (2017).

The mirrored stratigraphic positioning of the metasedimentary units from the southern Gilead, Maine 7.5’ quadrangle indicates the presence of a macroscopic D_2 refolded nappe structure. The center of the refolded nappe structure is comprised of the Rangeley Formation, and is located where the hinge lines of the D_2 Acadian folds are most easily identified. This feature is highlighted by the red line on figure 46. These stratigraphic correlations help to demonstrate that the study area lies on the inverted limb of the refolded nappe structure.

Previous Interpretations

Figure 47 displays a post depositional interpretation done by Watermulder (2014). Since the publication of her thesis, there have been a few updates to the understanding of the depositional basin of the Shapley group. Although the development of the olisostromal melange within the Rangeley formation is accurately represented, this figure inaccurately presents the depositional basin of the Rangeley stratigraphy as a forearc basin.

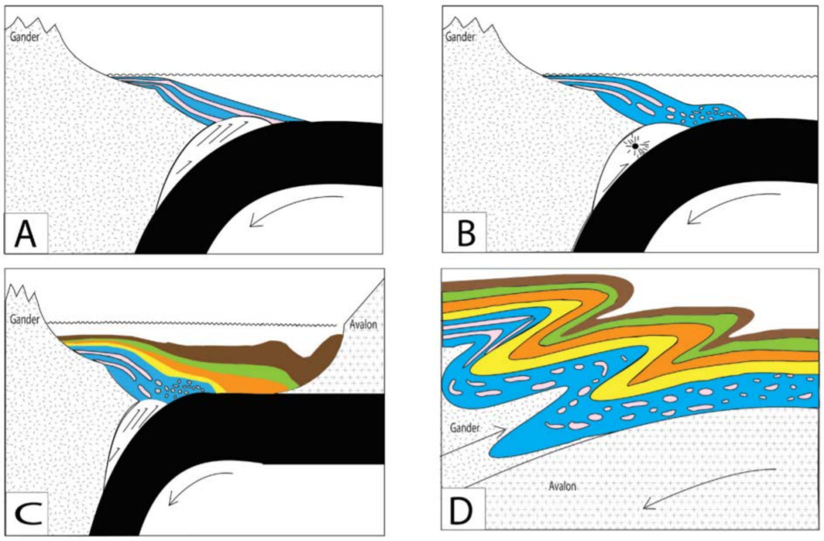

Figure 47. Post depositional sequence of events as interpreted by Sula Watermulder (2014).

This study believes that these members of the Rangeley stratigraphy were instead deposited in a retroarc basin within the Gander terrane based on interpretive paleo cross sections from previous studies (van Staal, 2009). Due to a lack of volcanic sediments contained within the Siluro-Devonian metasedimentary layers in the study area, it is unlikely that these units would have been deposited close to a subducting ocean plate. Previously discussed evidence from Solar and Tomascak (2016) suggested that the crustal source for the Late Devonian- Early Carboniferous S-type granites in the study area is part of the Bronson Hill belt, which is more extensive than previously thought. The magmatic event that was responsible for the intrusion of the S-type granites within the study area signals the end of the third phase of deformation, as there has been no foliation recognized within these granites. As was established by Bradley et al (2000) the welding of Avalon to the Laurentian craton was accompanied by flat slab subduction of the oceanic crust. Van Staal (2009) postulates that just east of the Red Indian Line, a portion of the Avalon oceanic crust broke off and descended into the mantle during the Late Devonian (figure 5). Evidence of the same Devonian-Carboniferous magmatic pulse within the study area emplaces the entirety of the Gilead, Maine 7.5' quadrangle on the Gander terrane during the progression of the Acadian, and subsequent Neoacadian orogenies.

Updated Post Depositional History

Based on the evidence from adjacent study areas and analysis of the data collected from the southern portion of the Gilead, Maine 7.5’ quadrangle, the following updated post depositional history was generated (Figures 48-50).

Early-Late Silurian (~450-423Ma.)

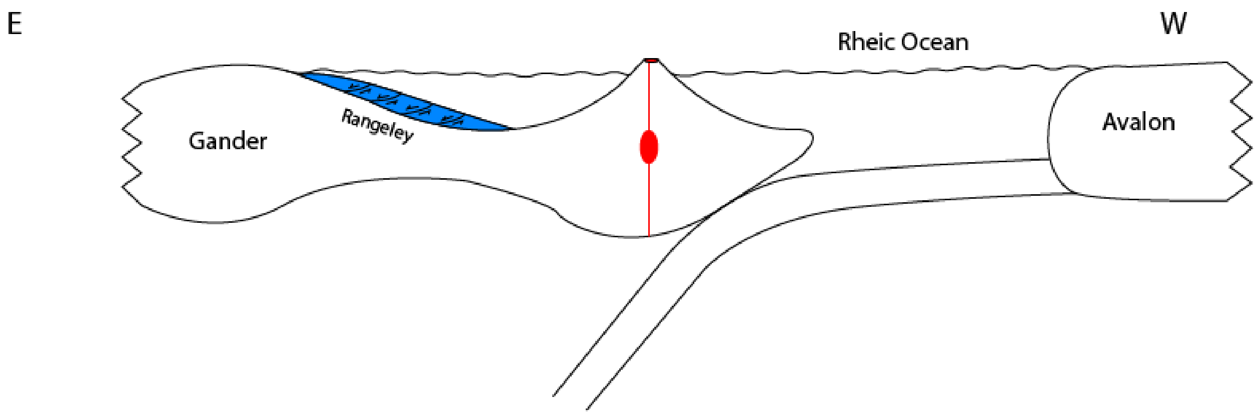

Figure 48. Early Silurian Salinic deformation. This coincides with the deposition of the Rangeley formation within a retroarc basin on Gander. There is active volcanism triggered on the outboard side of the basin by the subduction of ocean crust and approach of the ribbon continent Avalon. This subduction is likely also the source of the tectonic disruption that lead to the development of an olisostromal mélange (evidenced by calc-silicate pods) within the Rangeley Formation (Watermulder, 2014).

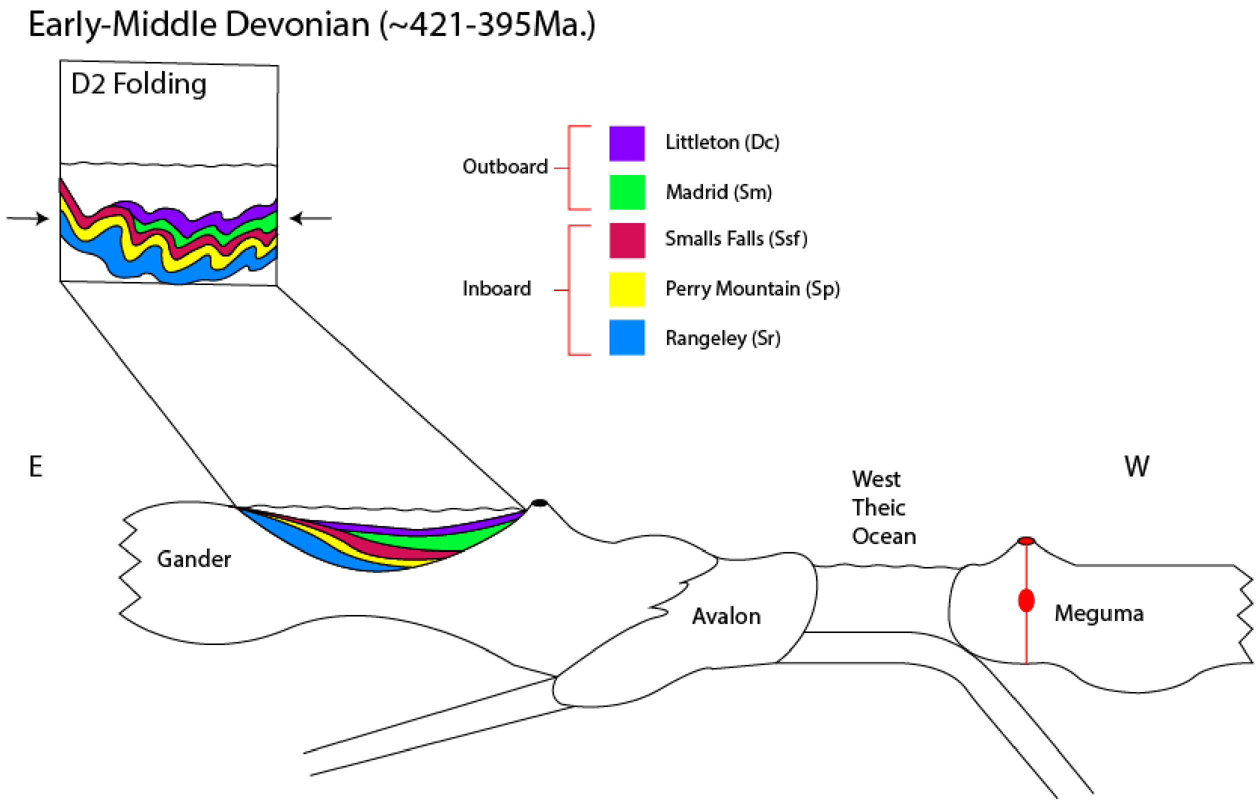

Figure 49. Early Devonian, Avalon has fully accreted to Gander and the remaining units that we have identified within the Gilead quad and other adjacent quads have been deposited. Closure of the retroarc basin has been initiated by the Acadian Orogeny, and the first major fold occurs here (F_2), as well as the establishment of the first schistocity (S_2). Formations defined as inboard are derived from the Gander side (West) of the retroarc basin, and outboard formations have eastern provenance. It is important to note the flat slab subduction of the ocean crust linked to Avalon. Inset shows effects of D_2 deformation on stratigraphic layers (Bradley et al, 2000).

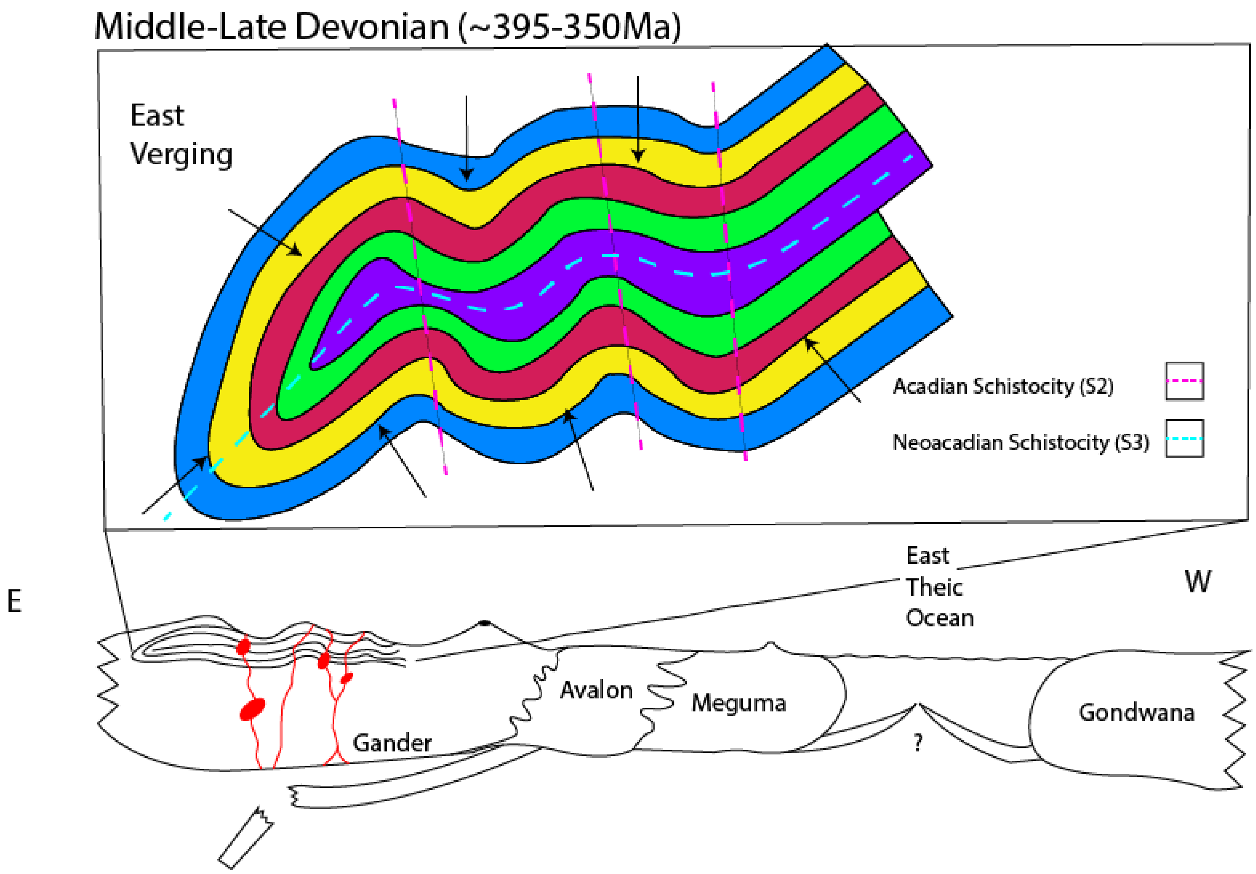

Figure 50. Frasnian, Meguma has been welded onto Avalon via backarc subduction and closure of the West Theic ocean. Neoacadian deformation develops within the remains of the retroarc at this time. At around 350Ma plutons are identified within the study area. These are likely responsible for the presence of large grained randomly oriented micas within some of the schist thin sections. This magmatic event was likely triggered by slab breakoff of the underriding oceanic slab connected to Avalon.

The fold system shown in the inset has been identified as East verging based on stratigraphic correlations made with adjacent quadrangles and graded beds from Mount Washington (Eusden et al, 1996). The antiformal structures within the Gilead quad are steeply inclined (axial plane avg dip: 74º; hinge line avg plunge: 54º). Acadian schistocity is shown here parallel with bedding at all regions but the hinge of the fold. Neoacadian schistocity is drawn where it would theoretically appear, however no examples of S_3 were found in the field due to previously discussed factors.

Conclusions

The bedrock geology of western Maine has experienced a complex sequence of folding and magmatic events related to tectonic and mountain building sequences that have moved throughout the Laurentian craton since the breakup of supercontinent Rhodinia. Various phases of folding and evidence of different terranes have been identified in Maine and New Hampshire. There are hundreds of millions of years of tectonic transport, deformation and partial melting contained within the rock records of New England.

Within the Gilead, Maine 7.5’ quadrangle, three phases of deformation were identified within a closed Gander retroarc basin. The Silurian and Devonian metasedimentary units within this basin showed evidence of Salinic (D_1) reverse faulting, Acadian (D_2) nappe scale isoclinal folding, and Neoacadian (D_3) ductile refolding. These three phases of deformation were bracketed by a combination of DZ and CZ dating of metasedimentary and igneous units from both the study area (Wheatcroft, 2017) and from relevant adjacent studies (Solar and Tomascak, 2016).

The identification of specific outcrop examples of deformation within the Gilead, Maine 7.5’ quadrangle, correlation of field structures with known phases of deformation that occurred during the Paleozoic, and subsequent timing of those deformational phases within the study area using the latest geochronology data available adds to the overall understanding of the rich and complicated deformational history of New England.

Further work will continue within regions in western Maine that have never been mapped at a 1:10000 scale. Greater access to outcrops due to logging and development since 1985 has made it possible to generate far more detailed mapping in western Maine and New Hampshire. These areas, including portions of the Bethel, Maine 7.5’ quadrangle, will add to the regional structural understanding of bedrock within the New England area.

References

Billings, M. P., and Fowler-Billings, K. (1975). The geology of the Gorham Quadrangle, New Hampshire and Maine. N. H. Dep. Res. Econ. Dev. Concord, N. H., Bull. 6, 120 p.

Bradley, D. C. and O'Sullivan, P. (2016). Detrital zircon geochronology of pre- and syncollisional strata, Acadian orogen, Maine Appalachians. Basin Res.

Bradley, D., & Tucker, R. (2002). Emsian synorogenic paleogeography of the maine appalachians. The Journal of Geology, 110(4), 483-492.

Bradley, D. C., & Geological Survey (U.S.). (2000). Migration of the acadian orogen and foreland basin across the northern appalachians of maine and adjacent areas. (No. no. 1624.;1624.;). Denver, CO;Menlo Park, CA;: U.S. Dept. of the Interior, U.S. Geological Survey.

Choe, Saebyul C., (2014). Petrographic Analysis and Tectonic Implications of the Plutons in the Gilead 7.5 Quadrangle: Connections to the Piscataquis Volcanic Arc and Sebago Batholith. Standard Theses. Paper 18.

De Yoreo, J. J., Lux, D. R., Guidotti, C. V., Decker, E. R., & Osberg, P. H. (1989). The acadian thermal history of western maine. Journal of Metamorphic Geology, 7(2), 169-190.

Eusden, J. D. & Eusden, R., (2013). Part of the Gilead Quadrangle, Maine. Maine Geological Survey.

Eusden, J. D. & Eusden R., (2013). Part of the Bethel Quadrangle, Maine. Maine State Geological Survey

J. Dykstra Eusden, J., Guzofski, C. A., Robinson, A. C., & Tucker, R. D. (2000). Timing of the acadian orogeny in northern new hampshire. The Journal of Geology, 108(2), 219-232

Fossen, H. (2010). Structural geology. Cambridge; New York;: Cambridge University Press.

Gibson, D., Barr, S.M., van Rooyen, D., White, C.E., (2017). Geochronology and geochemistry of granitoid plutons, Western Maine. Geological Society of America Abstracts with Programs. Vol. 49, No. 2

Hibbard J.P., van Staal, C.R., Rankin, D.W., Williams, H. (2006). Lithotectonic map of the Appalachian Orogen, Canada-United States of America. Geological Survey of Canada "A" Series Map. Issue 2096A

Hussey, A.M. II, (1989). Geology of Southwestern Coastal Maine. Maine Geological Survey, Neotectonics of Maine. Bowdoin Department of Geology

Konn, M.J., Spear, F.S., Valley, J.W., (1997). Dehydration-melting and fluid recycling during metamorphism: Rangeley Formation, New Hampshire, USA. Journal of Petrology; 38 (9)

Moench, R.H., and Boudette, E. L., (1970). Stratigraphy of the northwest limb of the Merrimack synclinorium in the Kennebago Lake, Rangeley. and Phillips quadrangles, western Maine, in Boone, G. M., ed., Guidebook for fie ld trips in the Rangeley Lakes - Dead River basin region, western Maine: 62nd New England Intercollegiate Geological Conference, p. D 1- 12.

Resnick, L. B., March, J. G., National Research Council (U.S.). Committee on Research in Mathematics, Science, and Technology Education, & National Research Council (U.S.). Commission on Behavioral and Social Sciences and Education. (1987). Education and learning to think. Washington, D.C: National Academy Press.

Osberg, P.H. (1978). Synthesis of the geology of the northeastern Appalachians, USA. Geological Survey of Canada, Paper 78-13, 137-147

Osberg, P. H., Hussey, A. M., II, and Boone, G. M. (1985). Bedrock geologic map of Maine. Dep. Conserv. Maine Geol. Surv. Augusta, Maine, scale 1: 500,000.

Press, Frank (2003). Understanding earth (4th ed). W. H. Freeman, New York, N. Y

Reusch, D.N., and van Staal, C.R., (2012). The Dog Bay – Liberty Line and its significance for Silurian tectonics of land: Canadian Journal of Earth Sciences, v. 37, p. 1691–1710

Solar, G.S and Tomascak, P.B., (2016). The Migmatite-Granite Complex of Southern Maine: Its Structure, Petrology, Geochemistry, Geochronology and Relation to the Sebago Pluton. in Berry, Henry N., IV, and West, David P., Jr., editors, Guidebook for field trips along the Maine coast from Maquoit Bay to Muscongus Bay: New England Intercollegiate Geological Conference, p. 19-42.

Taylor, B., (1997). Earth Explained. Marshall Editions. London, United Kingdom

Thompson, W. B., and Fowler, B. K., 1989, Deglaciation of the upper Androscoggin River valley and northwestern White Mountains, Maine and New Hampshire, in Tucker, R. D., and Marvinney, R. G., eds., Studies in Maine geology, Vol. 6, Quaternary geology: Augusta, Maine Geological Survey, p. 71-88.

Thompson, W., Eusden J. D., Breskin, K., (2014). Geology of the upper Androscoggin River region, Bethel, Maine, to Shelburne, New Hampshire. Geological Society of Maine and Geological Society of New Hampshire Summer Field Guide, 13.

Thompson, W. B., and Borns, H. W., Jr., 1985, Till stratigraphy and late Wisconsinan deglaciation of southern Maine: A review: Géographie physique et Quaternaire, v. 39, no. 2, p. 199-214.

Tomascak, P.B., and Solar, G.S., (2016). Anatomy of the migmatite-granite complex, southwestern Maine: Geological Society of America, Abstracts with Programs, v. 48.

Van Staal, C. R., Whalen, J. B., Valverde-Vaquero, P., Zagorevski, A., & Rogers, N. (2009). Pre-carboniferous, episodic accretion-related, orogenesis along the laurentian margin of the northern appalachians. Geological Society Special Publication, 327, 271-316.

Watermulder, Sula Q., (2014). Depositional Setting and Deformation History of Central-Western Maine: Silurian Stratigraphic Revisions for the Newry-Gilead Region. Standard Theses. Paper 17.

Welling, Douglass, S., (2001). The Stratigraphy and Structural Geology of the Northeast Flank of the Presidential Range, New Hampshire. Honors Thesis, Bates Department of Geology

Wheatcroft, A. (2017). Bedrock geology, stratigraphy and geochronology in the migmatite terrain of the southern Gilead, Maine 7.5’ quadrangle. Honors Thesis, Bates Department of Geology